VILNIUS GEDIMINAS TECHNICAL UNIVERSITY

ELECTRONICS FACULTY

ELECTRICAL ENGINEERING DEPARTMENT

Lukas Rimkus

TRACKING MAXIMUM POWER POINT OF PHOTOVOLTAIC MODULES UNDER NON-UNIFORM SOLAR IRRADIANCE

MASTER THESIS

TECHNOLOGICAL SCIENCES,
ELECTRICAL AND ELECTRONIC ENGINEERING (621H62002)

Supervisor: Dr. Prof. Nerija Žurauskienė

Head of the department: Dr. Prof. Vygaudas Kvedaras

Vilnius, 2014

VILNIAUS GEDIMINO TECHNIKOS UNIVERSITETAS
ELEKTRONIKOS FAKULTETAS
ELEKTROTECHNIKOS KATEDRA

TVIRTINU
Katedros vedėjas
_____
(Parašas)
_____
(Vardas, pavardė)
_____
(Data)

LUKAS RIMKUS

FOTOVOLTINIO MODULIO DIDŽIAUSIOS GALIOS TAŠKO NUSTATYMAS VEIKIANT NETIESINEI SAULĖS APŠVITAI

TRACKING MAXIMUM POWER POINT OF PHOTOVOLTAIC MODULES UNDER NON-UNIFORM SOLAR IRRADIANCE

Baigiamasis magistro darbas

Elektronikos ir elektros inžinerijos studijų kryptis
Elektros energetikos sistemų inžinerijos studijų programa, valstybinis kodas 621H62002
Elektros energetikos technologijų specializacija

Vadovas _____ _____ _____
(Moksl. laipsnis/pedag. vardas, vardas, pavardė) (Parašas) (Data)

Vilnius, 2014

VILNIAUS GEDIMINO TECHNIKOS UNIVERSITETAS
ELEKTRONIKOS FAKULTETAS
ELEKTROTECHNIKOS KATEDRA

Elektronikos ir elektros inžinerijos studijų kryptis
Elektros energetikos sistemų inžinerijos studijų programa, valstybinis kodas 621H62002
Moderniosios elektros energetikos inžinerijos specializacija

TVIRTINU
Katedros vedėjas

_____
(*parašas*)
Prof. dr. Vygaudas Kvedaras

BAIGIAMOJO MAGISTRO DARBO UŽDUOTIS

..... Nr. .....
Vilnius

Studentui Lukui Rimkui
(*vardas, pavardė*)

Baigiamojo darbo tema:

FOTOVOLTINIO MODULIO DIDŽIAUSIOS GALIOS TAŠKO NUSTATYMAS VEIKIANT NETIESINEI SAULĖS APŠVITAI
TRACKING MAXIMUM POWER POINT OF PHOTOVOLTAIC MODULES UNDER NON-UNIFORM SOLAR IRRADIANCE
(*lietuvių ir anglų kalbomis*)

patvirtinta 2012m. lapkričio mėn 11d. dekano potvarkiu Nr.299el

Baigiamojo darbo užbaigimo terminas 201... m. _____ mėn. ___ d.

BAIGIAMOJO DARBO UŽDUOTIES PRADINIAI DUOMENYS IR REIKALAVIMAI

Darbo tikslas: ištirti fotovoltinio modulio veikimo efektyvumą, kuriame yra įdiegtas didžiausios galios taško sekimo algoritmas.

Šiam tikslui pasiekti numatyti tokie uždaviniai:

1. Apžvelgti pagrindinius fotovoltinių modulių maksimalios galios algoritmus.
2. Sumodeliuoti fotovoltinio modulio sistemą.
3. Sukurti maksimalios galios nustatymo algoritmą.
4. Atlikti fotovoltinio modulio sistemos galios ir naudingumo skaičiavimus bei pateikti rezultatus.
5. Pateikti išvadas ir rekomendacijas.

Projekto vadovas: _____ Nerija Žurauskienė, dr. prof.
(*parašas*) (*vardas, pavardė, mokslinis vardas ir laipsnis*)

Užduotį gavau: _____ Lukas Rimkus
(*parašas*) (*vardas, pavardė*)

_____
(data)

Vilniaus Gedimino technikos universiteto egzaminų, sesijų ir baigiamųjų darbų rengimo bei gynimo organizavimo tvarkos aprašo 2011-2012 m. m.

1 priedas

(Baigiamojo darbo sąžiningumo deklaracijos forma)

VILNIAUS GEDIMINO TECHNIKOS UNIVERSITETAS

Lukas Rimkus,
20084441

(Studento vardas ir pavardė, studento pažymėjimo Nr.)

Elektronikos fakultetas

(Fakultetas)

Elektros energetikos sistemų inžinerija, EETfmu-12

(Studijų programa, akademinė grupė)

BAIGIAMOJO DARBO (PROJEKTO) SĄŽININGUMO DEKLARACIJA

2014 m. gegužės 29 d.

Patvirtinu, kad mano baigiamasis darbas tema „ fotovoltinio modulio didžiausios galios taško ieškojimas veikiant netiesiniai saulės apšvietai “ patvirtintas 2012 m. lapkricio 13d. dekano potvarkiu Nr. 299el, yra savarankiškai parašytas. Šiame darbe pateikta medžiaga nėra plagijuota. Tiesiogiai ar netiesiogiai panaudotos kitų šaltinių citatos pažymėtos literatūros nuorodose.

Mano darbo vadovas dr. prof. Nerija Žurauskienė

Kitų asmenų indėlio į parengtą baigiamąjį darbą nėra. Jokių įstatymų nenumatytų piniginių sumų už šį darbą niekam nesu mokėjęs (-usi).

	Lukas Rimkus
(Parašas)	(Vardas ir pavardė)

Abbreviations

I-V curves	Current and voltage characteristic
PV	Photovoltaic
SC	Solar cell
MPP	Maximum power point
MPPT	Maximum power point tracker
DC	Direct current
P&O	Perturb and Observe algorithm
MCU	Microcontroller unit
IncCond	Incremental conductance algorithm

Symbols

I_{ph}	Photocurrent or Light generated current
V_{pv}	Photocells output voltage
R_s	Series resistance of a solar cell
R_p	Parallel resistance of a solar cell
R_{mpp}	Load resistance at maximum power point
I_{sc}	Short circuit current
q	Electron charge
k	Boltzmann constant
T_C	Temperature of a solar cell
I_D	Dark saturation current
V_{oc}	Open circuit voltage
I_0	Reverse saturation current
G_a	Solar radiation
A	Area of the cell
P_{max}	Maximum power of the a solar cell
η_{max}	Power efficiency of a solar cell

Vilnius Gediminas Technical University

Faculty of Electronics

Department of Electrical Engineering

Electrical Energetics Systems Engineering study programme master thesis

TRACKING MAXIMUM POWER POINT OF PHOTOVOLTAIC MODULES UNDER NON-UNIFORM SOLAR IRRADIANCE

Author: Lukas Rimkus

Academic Supervisor: Dr. Prof. Nerija Žurauskienė

Thesis language – English

Annotation

This master work was focused on modelling and investigation of a photovoltaic module which operates in non-uniform solar irradiance and temperature changes which is typical to Lithuanian climate. 60 polycrystalline silicon cells were used to model photovoltaic module. *Matlab®/Simulink®* was used for modelling and calculating the whole system. To generate solar insolation curve, the latitude, longitude of the geographic place and a number of days in a year have to be selected. Buck-boost DC-DC converter and hill-climbing maximum power point tracking algorithm was used to produce maximum power point of the photovoltaic module. Modeled system has reached 93.95 % of maximum power from the photovoltaic module. Structure: introduction, review of maximum power point algorithms, system modelling, research results, conclusions, references. The thesis consists of: 60 pages, 41 figures, 16 tables, 37 references. Appendixes included.

Key words: Solar irradiance, photovoltaic module, maximum power point tracking, partial shading, DC-DC converter, *Matlab®/Simulink®*.

Vilniaus Gedimino Technikos Universitetas

Elektronikos fakultetas

Elektrotechnikos katedra

Elektros energetikos sistemų inžinerijos studijų programos baigiamasis magistro darbas.

FOTOVOLTINIO MODULIO DIDŽIAUSIOS GALIOS TAŠKO NUSTATYMAS VEIKIANT NETIESINEI SAULĖS APŠVITAI

Autorius: Lukas Rimkus

Vadovas: dr. prof. Nerija Žurauskienė

Kalba – anglų

Anotacija

Šiame magistro darbe buvo sumodeliuotas ir ištirtas fotovoltinio modulio veikimas, veikiant Lietuvoje būdingiems saulės apšvietos ir temperatūros pokyčiams. Fotovoltinį modulį sudaro 60 polikristalinių silicio celių sujungtų nuosekliai sistema. Modeliavimui ir skaičiavimas atlikti buvo naudojamas *Matlab®/Simulink®* programinės įrangos paketas. Įvedus vietos ilgumą, platumą ir pasirinkus metų dieną sugeneruojama saulės apšvietos kreivė paros bėgyje. Išgauti maksimalią galią iš fotovoltinio elemento buvo pasirinkta „buck-boost“ tipo įtampos keitiklis ir „Kalno-kilimo“ didžiausios galios taško algoritmas. Naudojant pasirinkto tipo įtampos keitiklį ir algoritmą galima pasiekti iki 93,95 % maksimalios galios. Darbą sudaro 7 dalys: įvadas, maksimalios galios algoritmų literatūros apžvalga, sistemos modeliavimas, maksimalios galios algoritmo sudarymas, rezultatai, išvados, literatūros sąrašas. Darbo apimtis 60 puslapiai, 2 priedai, 41 iliustracijų 16 lentelių, 37 bibliografiniai šaltiniai.

Raktiniai žodžiai: Saulės apšvita, fotovoltinis elementas, didžiausias galios taškas, šešėliavimas, įtampos keitiklis, *Matlab®/Simulink®*.

Content

1. Introduction

One of the barriers to the adoption of renewable energy technologies has been their relatively high cost. Policies of governments can be effective to promote renewable energy [1-3]. On the 11th of May, 2011 Lithuanian government approved renewable source energy law, which aim is to get 23 % of all energy production from renewable resources till 2020 [4]. In the case of solar power plant the aim is to get totally of 10 MW integrated electric power. Until January 2013 8.77 % is completed and a huge interest in less than 30 kW solar farms is apparent [5].

Such a phenomenon could be explained by a high tariffs acceptance of solar modules electrical energy. Many people took hasty to confirm their building requests for solar power plants, not fully consider how they can maximize the power of their system. In this work we will describe how electrical power extracted from solar modules could be maximized.

One of the most known solutions to boost electrical power from photovoltaic module is to use mechanism which can track sun's position in the real-time. There is a single axis mechanism that can move from east to west, and dual axis that can move from east to west and form north to south. In comparison of flat panel using single axis tracker generated power could increase by 27-40 % and dual axis – by 35-40 % [6]. Such systems that increase the amount of produced PV energy are called mechanical tracking systems [7-8].

Second, comparing with the countries in equatorial where PV modules can be pointed to Sun and it would generate almost full power, in mid-latitude Sun height is inconstant, there is more precipitations and because of that PV modules output voltage can fluctuate, as a result, it is hard to use this kind of electrical energy. To avoid such a negative phenomenon solar power plants must have power controllers, which could compensate or reduce voltage fluctuations or even cut off all noise.

Due to nonlinear I-V curves of PV cells, output power depends on intersection point of load line with this curve. For solar radiation and cell temperature values taken as examples, there is only one point where maximum power is produced. Therefore, operation of the cell at this point is the right option. This process is called an electrical maximum power point tracking or simply MPPT.

There are several methods that have been widely implemented to track the maximum power point (MMP). The most common methods are Perturb and Observe (P&O), incremental

conductance and three-point weight comparison [9]. Also, fuzzy logic MPPT method is highly used in the simulations of PV systems. In conclusions of paper Chin C. S *et al.* 'Optimization of fuzzy based maximum power point tracking in PV system for rapidly changing solar irradiance' [9] fuzzy logic MPPT system can track MPP faster than conventional MPPT even in variable changes of solar irradiance and fuzzy MPPT has the capability of reducing the perturbed voltage when MPP has been recognized.

2. Photovoltaic modules: maximum power point tracking methods (Literature review)

The general model of solar cell can be derived from an equivalent circuit named one diode model or single diode model [3]. It consists of photo current source, a diode, an equivalent parallel and series resistor, as shown in Fig. 2.1. Energy produced by photovoltaic cell is represented as ($I_{ph)}$ and it's proportional to solar radiation. The output voltage is ($V_{pv)}$. Serial resistance (R_s) is equal to the sum of contact and semiconductor material's resistances. Parallel resistance (R_p) is taken as the sum of resistances between thin-film layers and around cells. In the investigations, it is determined that parallel resistance is too large compared with series resistance, and its effect can be neglected.

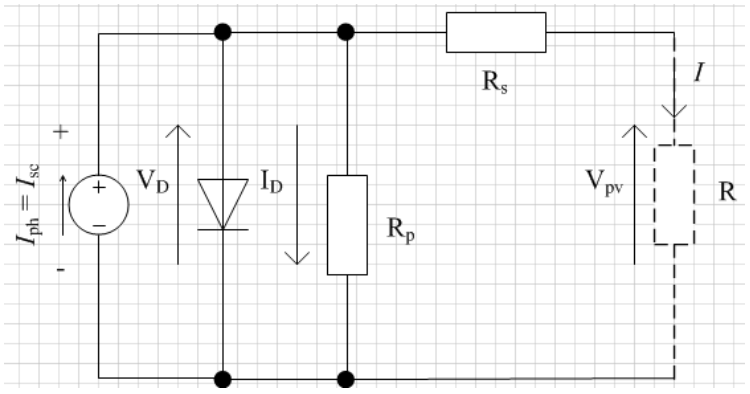

Figure 2.1. *One diode model represents solar cell*

When a load R is connected to the circuit current I will flow through. The output current will be short circuit and diode's current difference:

$$I = I_{sc} - I_D = I_{sc} - I_0\left(e^{(qV)/(kT_C)} - 1\right) \qquad (2.1)$$

Where q is electron charge $[1.6\cdot10^{-19}C]$, k is Boltzmann constant $[1.38\cdot10^{-23}(J/K)]$, T_C absolute temperature of solar cell [K], V voltage across the cell and I_D is the dark saturation current which varies depending on temperature of the cell, I_0 reverse saturation current. When the output current is zero the load voltage called open circuit voltage V_{oc} is:

$$V_{OC} = \frac{k \cdot T_C}{q} \ln \frac{I_{ph} + I_0}{I_0} \approx \frac{k \cdot T_C}{q} \ln \frac{I_{ph}}{I_0} \qquad (2.2)$$

As assumed V_{oc} and I_{ph} are important characteristics of solar cell and they are presented in all technical documentation of PV module manufactures [2-14]. Moving forward, we can describe the maximum power output P_{max} of solar cell and the power efficiency coefficient η_{max}.

$$P_{\max} = I_{\max} \cdot V_{\max}, \qquad (2.3)$$

$$\eta_{\max} = \frac{P_{\max}}{P_{in}} = \frac{P_{\max}}{A \cdot G_a}$$

Where A is an area of solar cell [m^2] and G_a is a solar irradiance [W/m^2]. Maximum power point can be seen from a graph below in Fig. 2.2, where current-voltage (I-V) and power-voltage (P-V) characteristics of a typical SC under variable solar irradiance conditions:

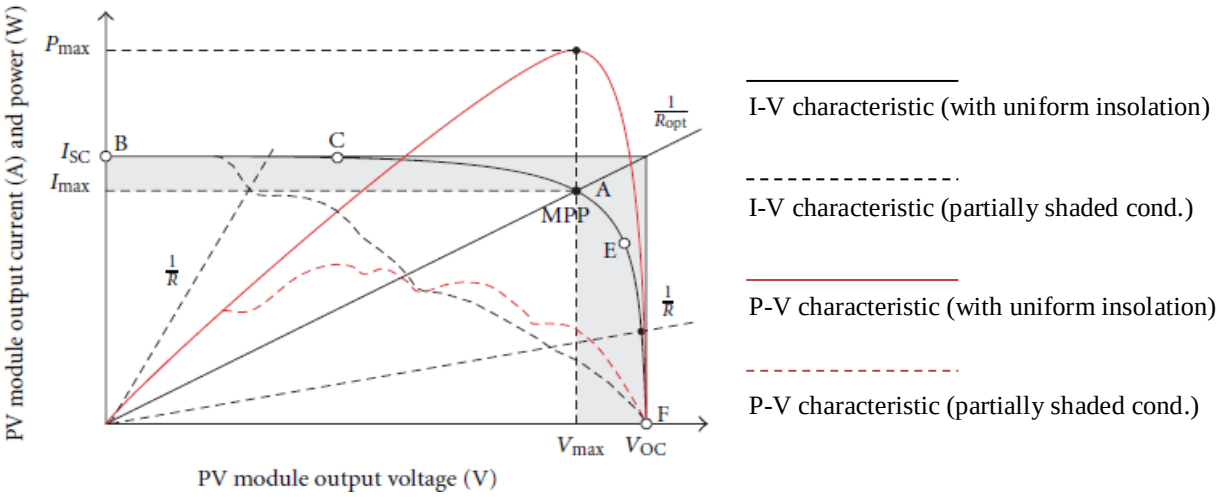

Figure 2.2. *Characteristics of typical solar cell* [7, 15-16]

In the graph above B-C line represents shorted circuit, when there is no load at the end of PV cell, and it will operate as a current source. If we connect the load to PV cell voltage will appear across it and PV cell will operate as a constant voltage source. Our aim is to get MPP in PV cell (A) where the highest efficiency of it is produced. Generally in non-uniform conditions (shading and temperature change), using MPPT quite considerable increases in output power by 20-30 % [7-17] could be achieved. The PV cell's I-V curves dependences on solar irradiation can be seen below in Fig. 2.3.

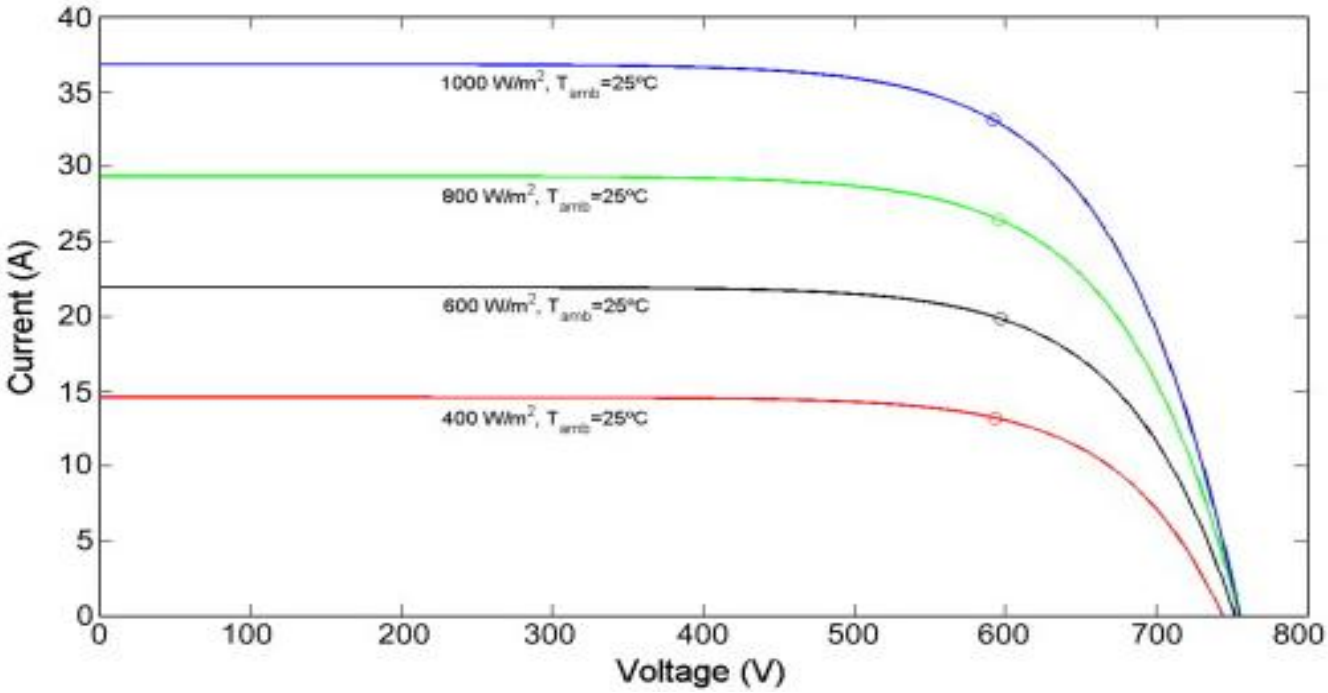

Figure 2.3. *I-V curves on different solar irradiation [18]*

In order to achieve the MPP in solar cell we will investigate methods that can track MPP, compare each method and present advantages and disadvantages.

In order to implement fuzzy logic controller or other control unit in PV cell, system must be configured. General system consists of a PV module, DC-DC converter, a load resistor and a single-chip control unit which is presented in Fig. 2.4.

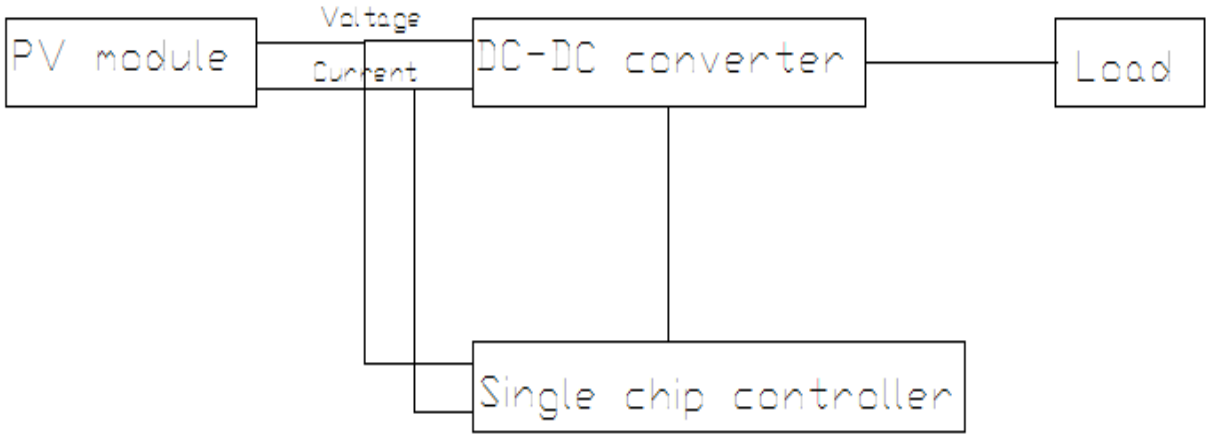

Figure 2.4.*Configuration of the PV system*

2.1. DC-DC converter topologies

Various research was performed over past two decades on DC-DC voltage converters. Study on non-isolated converters for photovoltaic applications [29] concisely reviewed various non-isolated DC-DC converters in order to help researcher to be able to choose the best converter. Converters have two tasks: interface a PV module and an output load such a grid or battery can drive the operating point of the PV module to the maximum power point. Converters are divided into categories of application, types of switching, current mode, etc. Frequently-used terms for DC-DC converters are non-isolated and isolated. "Isolation" refers to the electrical barrier separating the input and the output of a DC-DC converter.

DC-DC buck converter Fig. 2.5 (left), is a step down converter, where the output voltage magnitude is always lower than the input voltage magnitude, therefore buck converter is used for connecting high module voltages to low load or battery voltages. In DC-DC boost converter, where the output voltage magnitude is always higher than the input voltage magnitude, therefore, this converter is used to connect high load/battery voltages with low PV module voltages.

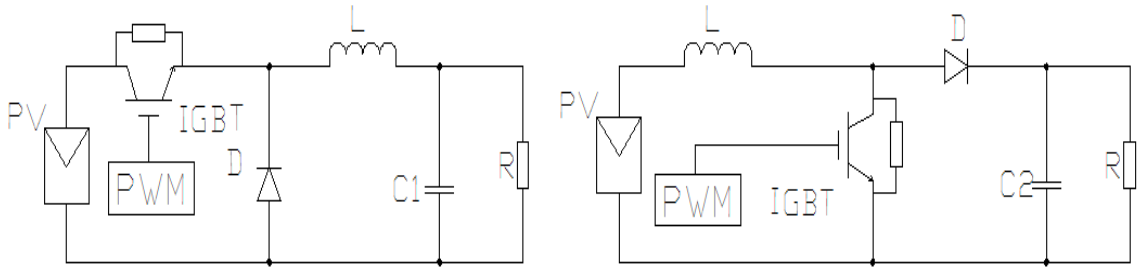

Figure 2.5. *Circuit of the buck (left) and boost (right) converters [24]*

The buck converter should be used with load impedance close to but less than R_{mpp} at the highest condition. However, the boost converter must be used with load impedance close but larger than R_{mpp} at lower conditions, with drawbacks of poor tracking behavior under low irradiation. At very low levels of insolation, for example, during heavy cloud cover, the power flow from PV module to battery may be reduced or stop completely because the MPP or open circuit voltage of the module may fall below that of the battery if a simple blocking diode is used. A buck converter would be similarly affected, however, a boost converter should always be able to extract the maximum power available from panel, even if it is low [30]. Voltage and resistance conversion ratios over duty cycle of a buck (2.2) and boost (2.3) converters are given below,

where V_{out} and V_{in} are the output and input voltage of the converter, respectively, and D is the duty cycle of the switch S [24].

$$\frac{V_{out}}{V_{in}} = D \qquad R_i = \frac{RI}{D^2} \tag{2.4}$$

$$\frac{V_{out}}{V_{in}} = \frac{1}{1-D} \qquad R_i = (1-D)^2 RI \tag{2.5}$$

DC-DC buck/boost converter Fig. 2.6, is a step-up-down, bi-directional converter, where the output voltage magnitude may be lower or higher than the input voltage magnitude, so this topology can be used in connecting nearly-matched battery or load and module voltages.

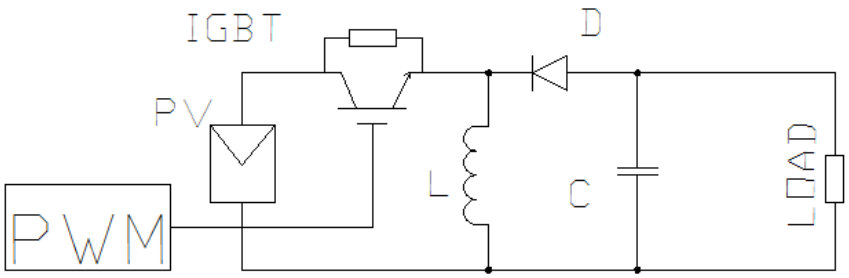

Figure 2.6. *Circuit diagram of a DC-DC buck-boost converter*

The duty ratio over input and output voltages and input resistance are the following:

$$\frac{V_{out}}{V_{in}} = \frac{1}{1-D} \qquad R_i = \frac{(1-D)^2}{D^2} RI \tag{2.6}$$

As operating in maximum power point, MPP can be set up anywhere on the I-V curve. Buck-boost DC-DC converter topology is the only one allowing follow-up of the PV module MPP regardless of a temperature, irradiance, and connected load, but the input current of a buck-boost topology is always discontinuous, so the current has many harmonic components producing high input ripple and significant noise problems. Practically the most effective topologies at any price is buck and boost. M.H. Taghvaee concluded that the best type of converter for PV system is the buck-boost DC-DC converter [18]. This converter should be able to ensure optimum MPPT operation for any solar irradiation, cell temperature and load conditions.

2.2. Maximum power point tracking methods

There are many methods that been investigated on tracking MPP over decade. For example, in the application report of 'Introduction to Photovoltaic Systems Maximum Power Point tracking' [20] D. Freeman from Texas instrument compares five different methods:

1. Constant Voltage
2. Open Circuit Voltage
3. Short Circuit Current
4. Perturb and Observe
5. Incremental Conductance

Author concludes that in general, for whatever method that is chosen, it is better to be accurate than fast. Fast methods tend to bounce around the maximum power point due to noise. At low levels of irradiation Open Circuit Voltage and Short Circuit Current may be more appropriate as they can be more immune to noise. When the cells are arranged in a series, the iterative methods can be a better solution. When a portion of the string is shade or does not have the same angle of incidence, then searching algorithms are needed.

In the paper 'Comparison of Photovoltaic Array Maximum Power Point Tracking Techniques' [21] authors investigate different MPPT techniques that are in present and compares them in a well-organized table below:

Table I
Major characteristics of MPPT

MPPT technique	**PV Array Dependent**	**True MPPT**	**Analog or Digital**	**Periodic Tuning**	**Convergence Speed**	**Implementation Complexity**	**Sensed Parameters**
Hill-climbing /P&O	NO	YES	BOTH	NO	VARIES	LOW	VOLTAGE, CURRENT
IncCond	NO	YES	DIGITAL	NO	VARIES	MEDIUM	VOLTAGE, CURRENT
Fractional V_{OC}	YES	NO	BOTH	YES	MEDIUM	LOW	VOLTAGE
Fractional I_{SC}	YES	NO	BOTH	YES	MEDIUM	MEDIUM	CURRENT
Fuzzy Logic Control	YES	YES	DIGITAL	YES	FAST	HIGH	VARIES
Neural Network	YES	YES	DIGITAL	YES	FAST	HIGH	VARIES
Ripple correlation control	NO	YES	DIGITAL	YES	FAST	HIGH	VOLTAGE, CURRENT

Current Sweep	YES	YES	DIGITAL	YES	SLOW	HIGH	VOLTAGE, CURRENT
DC Link Capacitor Droop Control	NO	NO	BOTH	NO	MEDUIM	LOW	VOLTAGE
Load *I* or *V* Maximization	NO	NO	ANALOG	NO	FAST	LOW	VOLTAGE, CURRENT
*dP/dV*or*dP/dI*Feedback Control	NO	YES	DIGITAL	NO	FAST	MEDIUM	VOLTAGE, CURRENT
Array Reconfiguration	YES	NO	DIGITAL	YES	SLOW	HIGH	VOLTAGE, CURRENT
Linear Current Control	YES	NO	DIGITAL	YES	FAST	MEDIUM	IRRADIANCE
I_{MPP} & V_{MPP} Computation	YES	YES	DIGITAL	YES	N/A	MEDIUM	IRRADIANCE, TEMPERATURE
State-based MPPT	YES	YES	DIGITAL	YES	N/A	HIGH	VOLTAGE, CURRENT
OCC MPPT	YES	NO	BOTH	YES	FAST	MEDIUM	CURRENT
BFV	YES	NO	BOTH	YES	N/A	LOW	NONE
LRCM	YES	NO	DIGITAL	NO	N/A	HIGH	VOLTAGE, CURRENT
Slide Control	NO	YES	DIGITAL	NO	FAST	MEDIUM	VOLTAGE, CURRENT

Some of MPPT techniques presented in Table I, are specific in a way that they operate in a circuit connected only in one way. For example, DC link capacitor droop control is specifically designed to operate with a PV system that is connected in parallel with an AC system line [21]. The criterions in choosing MPPT technique are very wide. For simulation software like *MATLAB/Simulink* of PV system it is better to choose neural networks, IncCond. If using of software or programming microcontrollers is necessary, digital techniques would be more useful. Fuzzy logic control technique could be preferred for systems that requires fast convergence speed. Such system could be solar vehicles, where the load consists mainly of batteries.

2.2.1. Fuzzy logic control technique

Fuzzy logic consist of 4 stages: fuzzification, rule base, inference engine and defuzzification. In the case of MPP the inputs to a fuzzy logic controller are an error E and a change in error ΔE and it uses the approximation [21-22]:

$$E(n) = \frac{P(n) - P(n-1)}{V(n) - V(n-1)} \qquad 2.7.$$

and

$$\Delta E(n) = E(n) - E(n-1) \qquad 2.8.$$

In the stage of fuzzification the numerical inputs are turned in linguistics such as: NH (negative high), NL (negative low), Z (zero), PL (positive low), PH (positive high). System with more inputs probably will have better accuracy. Member functions as in Fig. 2.7 can be less symmetrical for one or the other variable importance. When E and ΔE are known, they are converted to linguistic variables, the fuzzy logic controller output – duty ratio ΔD of the power converter, can be found from a rule base table II. Esram T., Chapman P. L. concludes that fuzzy logic control algorithm is well suited under varying atmospheric conditions, as in mid-latitude zone. The disadvantage of this method could be that the effectiveness depends on the knowledge of the user or system engineer in choosing the right error computation and coming up with the rule base table.

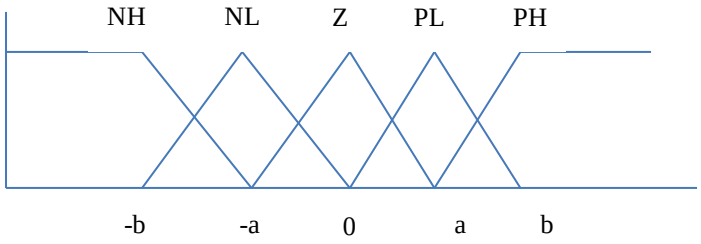

Figure 2.7. *Member functions for inputs and output of fuzzy logic controller [20]*

Table II

Fuzzy rule base table

$E / \Delta E$	**NH**	**NL**	**Z**	**PL**	**PH**
NH	**Z**	**Z**	**NH**	**NH**	**NH**
NL	**Z**	**Z**	**NL**	**NL**	**NL**
Z	**NL**	**Z**	**Z**	**Z**	**PL**
PL	**PL**	**PL**	**PL**	**Z**	**Z**
PH	**PH**	**PH**	**PH**	**Z**	**Z**

Fuzzy logic control is based on microcontrollers and its popular use is apparent in MPPT over the last decade. It's very helpful when inputs are not very precise, not needing an accurate mathematical model and handing nonlinearity.

The fuzzy logic algorithm is based on the following rule: "If the last change in the duty-cycle (duty-ratio ΔD) has caused the power to raise, keep moving the duty-cycle in the same direction; otherwise, if it has caused the power to drop, move it in the opposite direction" [23-24]. In the work of 'Design and Implementation of A Fuzzy Logic Based A Photovoltaic Peak Power Tracking Controller' authors [23] are using MC9S12DP256B MCU for fuzzy logic implementation into photovoltaic system and they concluded that "the tracker efficiency reached up to 99.9% under different sudden change irradiance level and the system is found to have good stability at MPP".

2.2.2. *IncCond* technique

In the work of 'Investigation and improvement of electronic control system for solar energy sources' [3] author (Vasarevičius D.) is testing *IncCond* (Incremental conductance) algorithm. The algorithm can be presented with approximations below:

$$\frac{dI}{dU} \approx \frac{\Delta I}{\Delta U} \pm \zeta, \qquad 2.9.$$

$$\Delta I = I_{[i]} - I_{[i-1]}, \qquad 2.10.$$

$$\Delta U = U_{[i]} - U_{[i-1]}, \qquad 2.11.$$

Where: ΔI and ΔU - currents and voltages change in 1 s, ζ - error. From testing it was proven that the size of the error is limited by load resistance size when solar irradiation (S) is decreasing, that's why it's taken in respect with the lowest value of S, from which system starts to operate.

The author [3], after 25 tests of *IncCond* algorithm, concluded: when climate is stable, algorithm works fine and finds MPP after 400s; when load resistance step is high ($\Delta R = 2\Omega$) photovoltaic system reaches near MPP after 10s, but because of very sensitive system from irradiation algorithm doesn't hit the right MPP and it fluctuates around it, because of that system outputs big electromagnetic noise. It's a negative impact for the efficiency of the system; when the step size of the load resistance is small ($\Delta R = 0.1\Omega$), it takes more time (140 s) to reach

MPP, but because of that system became more stable and constant at MPP; after 25 test was concluded that dynamically changing solar irradiation, MPPT efficiency could drop to 83 % and the efficiency of *IncCond* algorithm is limited to 95 % because of variable dependence.

2.2.3. Neural Network

Neural networks commonly have three layers: input, hidden, and output layers as shown in Fig. 2.8. The number of nodes in each layer vary and are user-dependent. The input variables can be PV array parameters like V_{OC} and I_{SC}, atmospheric data like irradiance and temperature, or any combination of these. The output is usually one or several reference signal(s) like a duty cycle signal used to drive the power converter to operate at or close to the MPP.

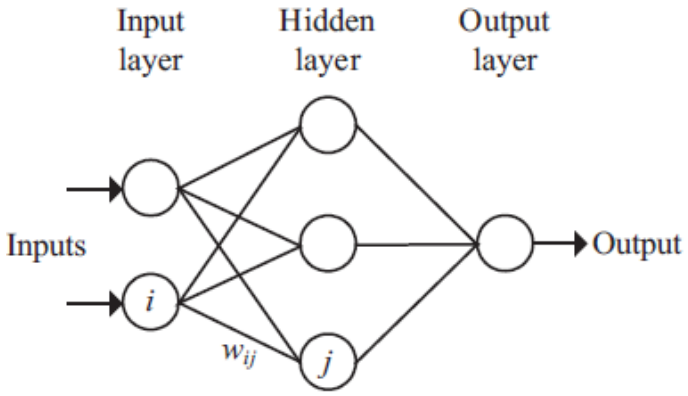

Figure 2.8. *Example of neural network [3]*

An imitation software in *Matlab*®*/Simulink*® environment, which is presented in Fig. 2.9, has been made in [3]. To imitate real solar irradiation over Lithuanian climate, it was used original cloudy weather model. After repeated tests the author concluded that system efficiency the first day is 97 % and all others ~99 %.

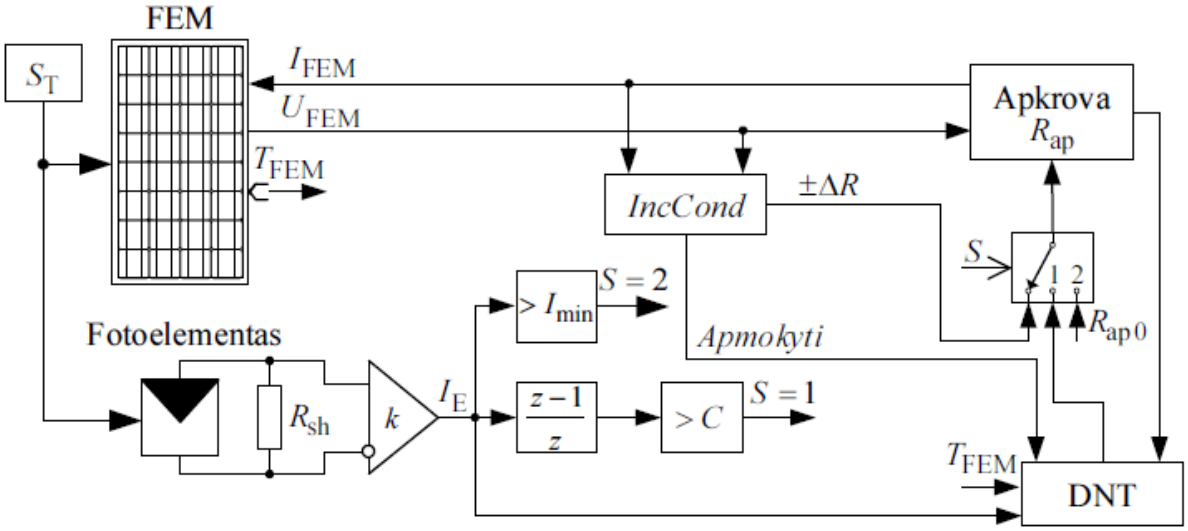

Figure 2.9. *Structure diagram of maximum power point tracking system with on-line learning artificial neural network [2]*

This model can use small steps of load resistance (ΔR = 0.3 Ω), in respect the system will avoid high power fluctuations when solar irradiation is very intense and it will not lose stability over low irradiation.

2.3. Conclusions

This literature review represents the description of system that could be implemented in PV module for MPPT. The major characteristics of techniques of MPPT are presented in Table I. It is shown that for Lithuanian climate three considered techniques could be adapted: Fuzzy logic control, IncCond and neural networks algorithms. IncCond algorithm showed efficiency of over 95 %, Fuzzy logic control – ~99.9 % and Neural Network – 99 %. All these techniques use digital implementation on a single-chip controller as presented in Fig. 2.4. Taking into account the reviewed results presented in literature, the solar irradiance, PV module, DC-DC converter will be simulated as a standalone system for further research.

3. Structural model design

3.1. Directed solar irradiation simulation

Scientists utilize the average distance from the Earth to the Sun (*D*) as the standard for one astronomical unit (1 AU). This average distance from the Earth to the Sun is 149,597,870.691 km [26]. To approximate solar irradiation at a given day we have to take this phenomenon into consideration. Within this approach the extraterrestrial solar irradiation is described [34] as:

$$S(n) = S_0\left(\frac{D}{D_0}\right)^2 \qquad 3.1.$$

Where $S(n)$ - solar irradiation of particular day; S_0 - average annual solar irradiation that hits Earth (Sun`s constant) 1367 W/m^2; *D* - average distance from the Earth to the Sun; D_0 - distance from the Earth to the Sun at a particular day in the year. The parameter $\left(\frac{D}{D_0}\right)^2$ is called eccentricity correction coefficient ε. In the work of '*Solar energy fundamentals and modeling techniques: atmosphere, environment, climate change and renewable energy'* [27] the eccentricity, ε, correction factor of the earth's orbit is described as:

$$\begin{aligned}\varepsilon = 1.00011 + 0.034221\cos\Gamma + 0.00128\sin\Gamma = \\ + 0.000719\cos 2\Gamma + 0.000077\sin 2\Gamma\end{aligned} \qquad 3.2.$$

Where day angle Γ, in radians given by:

$$\Gamma = \frac{2\pi(N-1)}{365} \qquad 3.3.$$

Where *N* presents day in a year (January 1, *N* = 1; December 31, *N* = 365). Figure 2.1 shows Earth`s orbit around the Sun. Around July 5th Earth is in aphelion state – the longest distance from Earth to Sun and in the beginning of January in perihelion state – the nearest distance from

Earth to Sun [19]. For this, on the Northern Hemisphere summers are colder and winters are warmer.

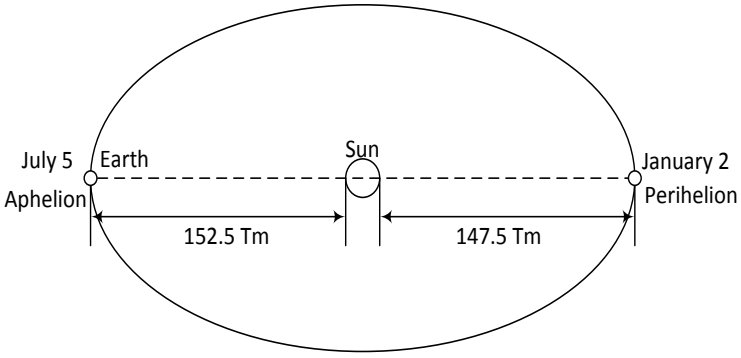

Figure 3.1. *Earth`s orbit around the sun*

The extraterrestrial solar radiation model designed in *Matlab®/Simulink®*. Figure 3.2 shows the results of 3.1 – 3.3 equations. The extraterrestrial solar radiation:

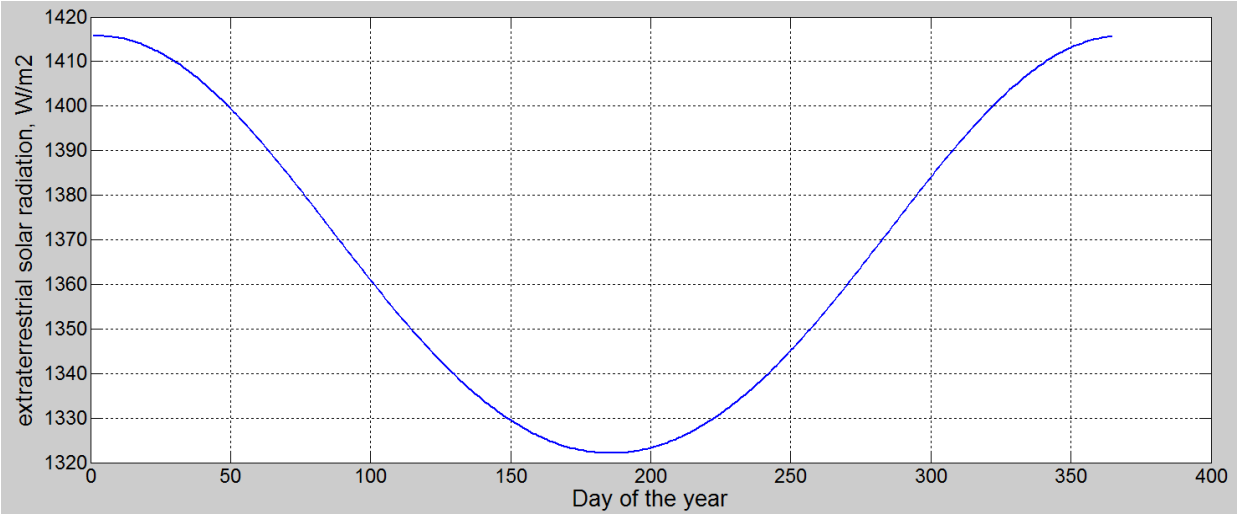

Figure 3.2. *Annual extraterrestrial solar radiation over the Earth*

When solar irradiation reaches Earth`s atmosphere, a part of solar irradiation is absorbed, diffused and reflected by inner troposphere. Figure 3.3 shows the phenomena of solar power flux that reaches the Earth`s ground. Travelling through the atmosphere part of solar rays is absorbed, reflected and scattered. The Direct irradiation that hits directly to the Earth`s ground plane is calculated by 3.4 formula:

$$S_{dir} = S(n) \cdot \tau \cdot \cos\theta_z \qquad 3.4.$$

Where θ_z - the zenith angle between solar beam and zenith. τ – atmospheric transmittance for beam radiation, which is exponentially decreasing form depending on the altitude and zenith angle θ_z as.

$$\tau = a + b\exp\left(-\frac{c}{\cos\theta_z}\right) \qquad 3.5.$$

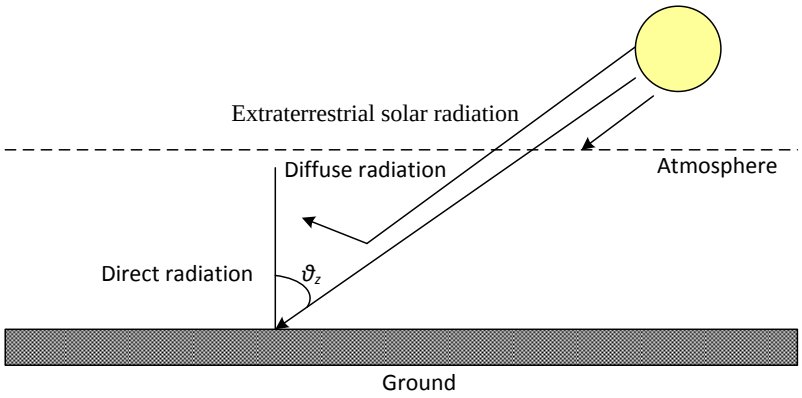

Figure 3.3. *Solar power flux falling to the ground*

where the estimations of constants a, b, and c for the standard atmosphere with 23 km visibility are given for altitudes less than 2.5 km by:

$$a = 0.4237 - 0.00821(6 - A)^2 \qquad 3.6.$$

$$b = 0.5055 - 0.005958(6.5 - A)^2 \qquad 3.7.$$

and $$c = 0.2711 - 0.01858(2.5 - A)^2 \qquad 3.8.$$

Where A is the high above sea level. In the work '*Investigation and Improvement of Electronic Control System for Solar Energy Sources'* [2] hourly atmospheric transmittance for Lithuania's climate conditions are estimated by using data from Kaunas meteorological station. In this case the high A is constant and τ*:*

$$\tau = 0.1365r_0 + 0.7507r_1\exp\left(\frac{0.3795r_k}{\cos\theta_z}\right) \qquad 3.9.$$

Where r_0 = 1.95, r_1 = 0,8102ir r_k = 0.6155. The angles of zenith θ_z and altitude β depends on the location point in which the solar irradiation hits the ground, geographical coordinates, the distance from equator δ (declination angle):

$$\cos\theta_z = \left(\frac{\pi}{2} - \beta\right) = \sin\beta, \qquad 3.10.$$

$$\cos\theta_z = \sin\beta = \cos(\phi_{LA})\cos(\Delta\phi_M)\cos(\delta) + \sin(\phi_{LA})\sin(\delta), \qquad 3.11.$$

Where ϕ_{LA} - latitude angle of point A, rad, $\Delta\phi_M$ - difference of midday and location meridian angle, rad, δ - declination angle, rad. To calculate declination angle in rad [5]:

$$\delta = 0.4093\sin\left[\frac{2\pi(n-81)}{365}\right]. \qquad 3.12.$$

Fig. 3.4 shows δ change from January 1st to December 31th.

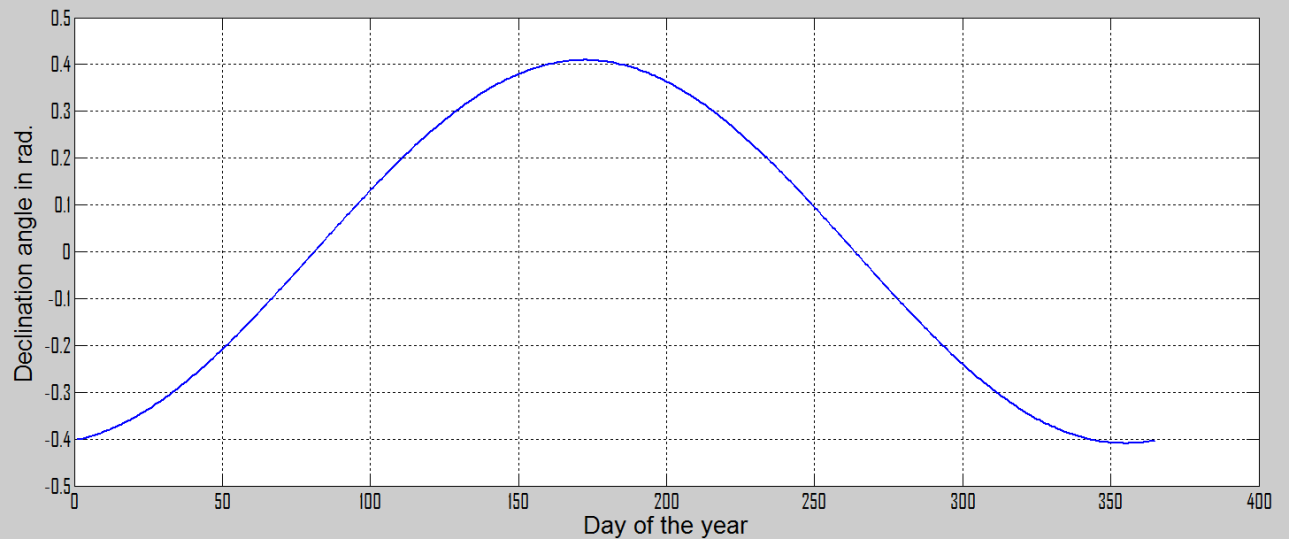

Figure 3.4. *Declination angle δ overall year*

Within a day the angle of $\Delta\phi_M$ changes over 2π, for this reason $\Delta\phi_M$ is written:

$$\Delta\phi_M(t_{ST}) = \omega(12 - t_{ST}), \qquad 3.13.$$

Where $\omega = \pi/12$ - earth rotation speed of its axis, rad/h, 12 – the midday value, h, t_{ST} - sun (location) time, [0.24], h. Until midday $0 \le t_{ST} \le 12$ and $\Delta\phi_M$ values are positive, after midday $12 \le t_{ST} \le 24$, $\Delta\phi_M$ are negative. To separate day and night time, the angle of zenith θ_z must be below $\pi/2$, $0 \le \theta_z \le \pi/2$, the mathematical description:

$$S_{dir}(n)=\begin{Bmatrix} S(n)\tau\cos\theta_z, & 0\le\theta_z\le\pi/2 \\ 0 & else \end{Bmatrix} \qquad 3.14.$$

Solar and zone time relationship:

$$t_{ST}=t_{CT}-\Delta t_{CTi}+\nu_{ST}(\phi_{MTZ}-\phi_{MA})+\Delta t_{\varepsilon}(n), \qquad 3.15.$$

Here: Δt_{CTi} - summer time correction, *h*. In Summer, $\Delta t_{CTi}=1$one hour forward, and in winter $\Delta t_{CTi}=0$. $\nu_{ST}=1/15$ solar time in time zone changing speed, $^{o}/h$, ϕ_{MTZ} - time zone meridians geographical longitude, ^{o}, $\Delta t_{\varepsilon}(n)$- correction of solar position in midday depending on rotation in elliptic orbit *n*-day of the year. The $\Delta t_{\varepsilon}(n)$ approximation:

$$\Delta t_{\varepsilon}(n)=0.165\sin\left[2\frac{2\pi(n-81)}{365}\right]-0.126\cos\left[\frac{2\pi(n-81)}{365}\right]- 0.025\sin\left[\frac{2\pi(n-81)}{365}\right]. \qquad 3.16.$$

Fig. 3.5 shows $\Delta t_{\varepsilon}(n)$ change from January 1st to December 31th.

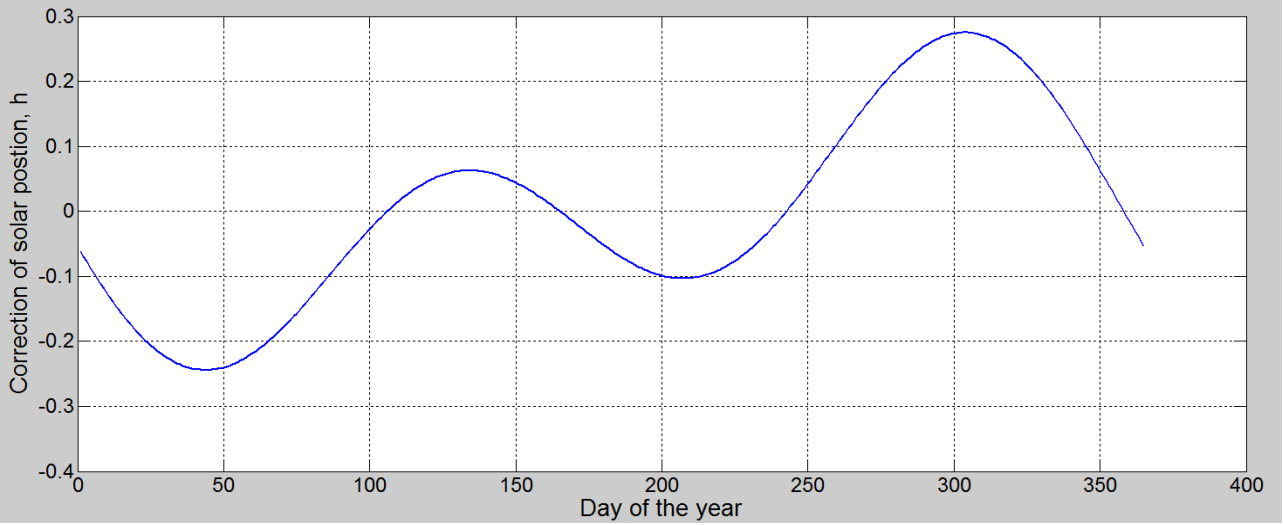

Figure 3.5. $\Delta t_{\varepsilon}(n)$ *during the year*

Using the calculations above, Fig. 3.6 shows (3.11) formula in a graphical view. It is good to change the angle θ_z into angle of sun's altitude β by using (3.10) and (3.11) formulas and arcsin(sin β). Assuming that Vilnius area is in 54°40′40″N 25°17′30″E [6]

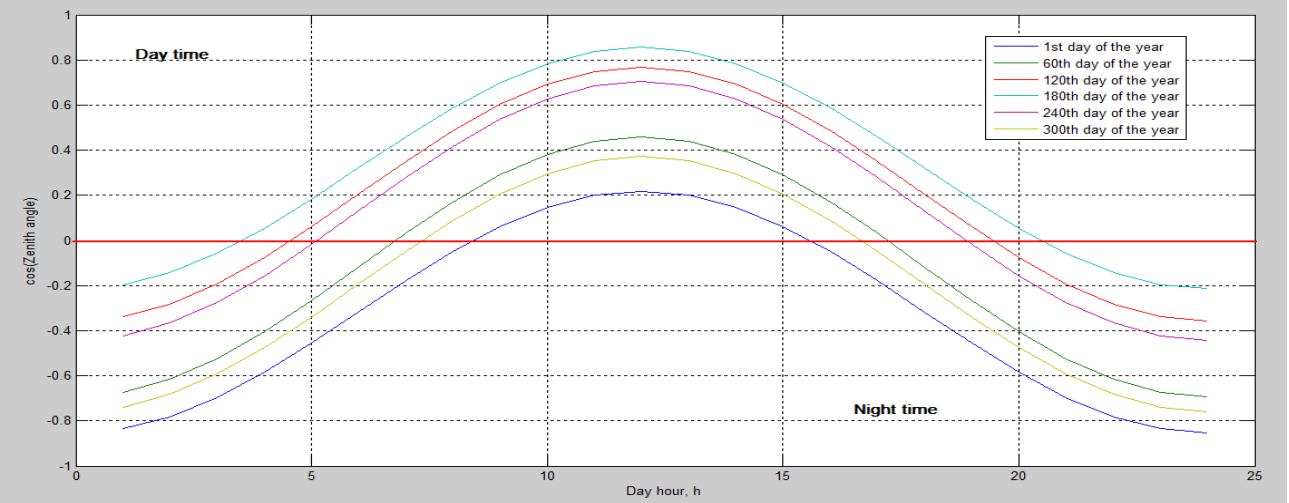

Figure 3.6. *Shows Zenith angle ϑ_z on a different day of the year*

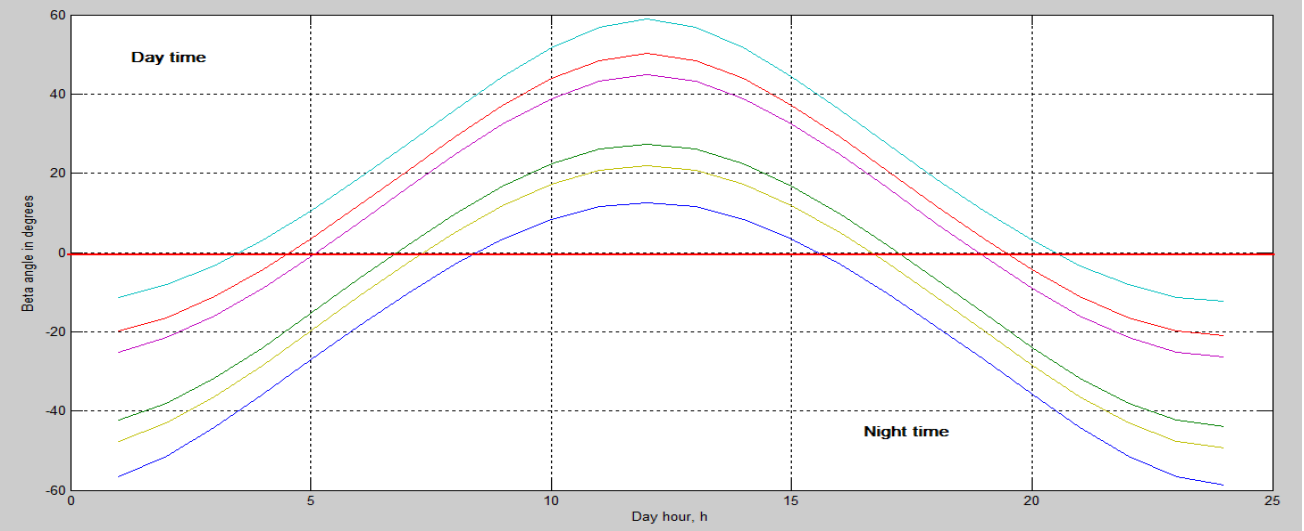

Figure 3.7. *Angle of sun's altitude β on a different day of the year*

Using (3.4) and (3.14) formulas, the directed solar irradiation onto the ground on a specific place and date in earth is calculated and it's show in Fig. 3.8. In the graph below 200th day of the year is picked, which is usually July 18th. Looking in a graph below it is easy to assume that the total energy of the day and year would be area plot below line, which is:

$$E_{dir} = \int_{t1}^{t2} S_{dir} dt \,,\; E_{year} = \sum_{i=1}^{n=365} E_{dir} \qquad 3.17.$$

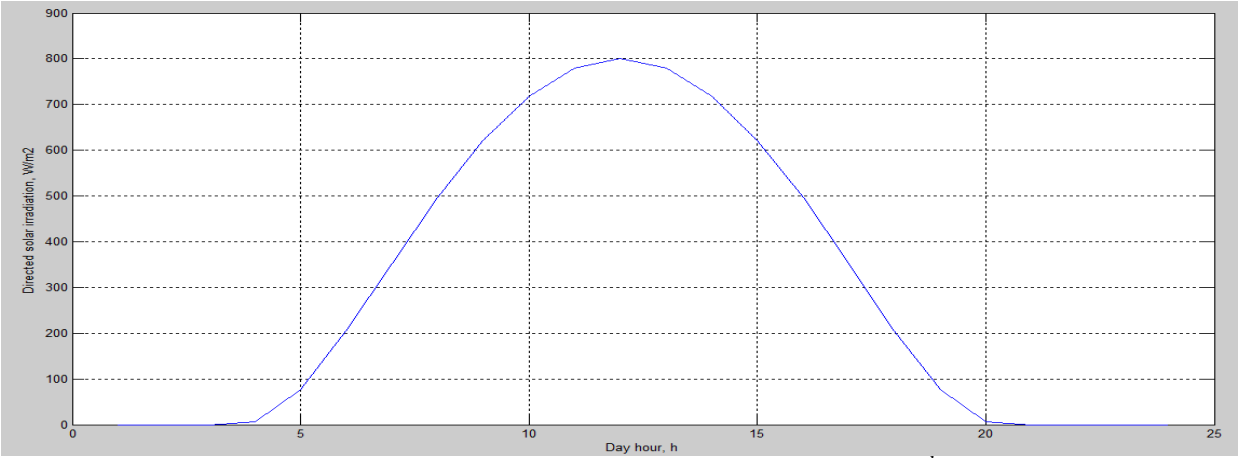

Figure 3.8. *Simulated directed solar irradiation in July 18th in Vilnius*

3.2. Total amount of solar irradiation simulation

Calculated directed solar irradiation is not the only one light source that hits the photovoltaic panels. When extraterrestrial solar irradiation enters Earth's atmosphere it's divided into directed, diffused and reflected solar irradiations. Diffused solar irradiation S_{dif} usually appears when the light hits a cloud, the water particles inside a cloud reduces the energy of atmospheric irradiation and then, in various directions, diffused solar irradiation hit the surface of the Earth. The approximation of S_{dif} :

$$S_{dif}(n) = \tau_{dif} \cdot S(n) \cdot \cos\theta_z \cdot \left(\frac{1+\cos\varphi}{2}\right), \qquad 3.18.$$

Where τ_{dif} - diffused atmospheric transmittance, φ - is the angle between solar panel and the horizontal ground, τ_{dif} is related with τ :

$$\tau_{dif} = 0.271 - 0.294\tau, \qquad 3.19.$$

Reflected solar irradiation S_{ref} is the irradiation that depends on both atmospheric transmittance, directed solar irradiation and the albedo of the ground. Albedo is a reflection coefficient that shows how much of energy is left in the light beam when it hits the surface. For example, highest albedo rate could be found in north or south poles, because of the white clean snow albedo is 0.85. It could be from 0.15-0.3 where we have green grass. The S_{ref} is as follows:

$$S_{ref}(n) = \rho \cdot S(n) \cdot \cos\theta_z \left(\tau + \tau_{dif}\right) \cdot \left(\frac{1+\cos\varphi}{2}\right), \qquad 3.20.$$

Where ρ - albedo of the surface. Having all the solar irradiations that could possibly influence photovoltaic panel we could calculate the total solar irradiation that hits the surface of ground:

$$S_{\sum}(n) = S_{dir}(n) + S_{dif}(n) + S_{ref}(n).\,, \qquad 3.21.$$

Fig. 3.9 shows $S_{\sum}$ and compares with other irradiations:

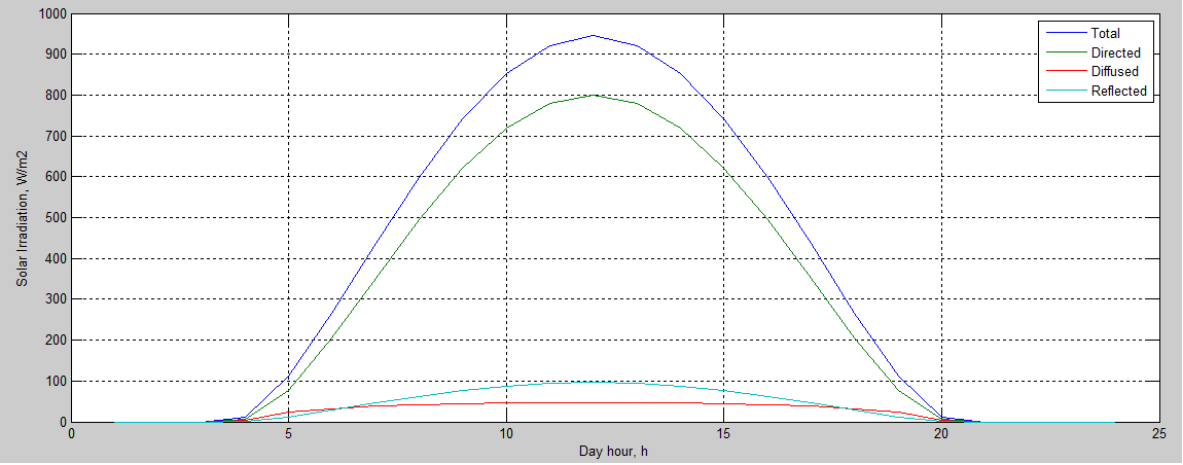

Figure 3.9 *All solar irradiations calculated that hits on a surface at Vilnius area in July 18th .*

3.3. Simulation of a cloudy day

There are two possible solutions to represent cloudiness: the first is to use mathematical approach and yearly statistics about daily weather; the second to make variable that could be possible to change for closer and use real-time simulation to see when the model of weather is very near to the real one. In Fig. 3.10 (top) illustrated real solar irradiation, which data was gathered in Kaunas and Šilutė meteorological stations with pironometer. In Fig. 3.10 (bottom) presents simulated total solar irradiance when shaded coefficient is implemented. The coefficient is described in Appendix A.

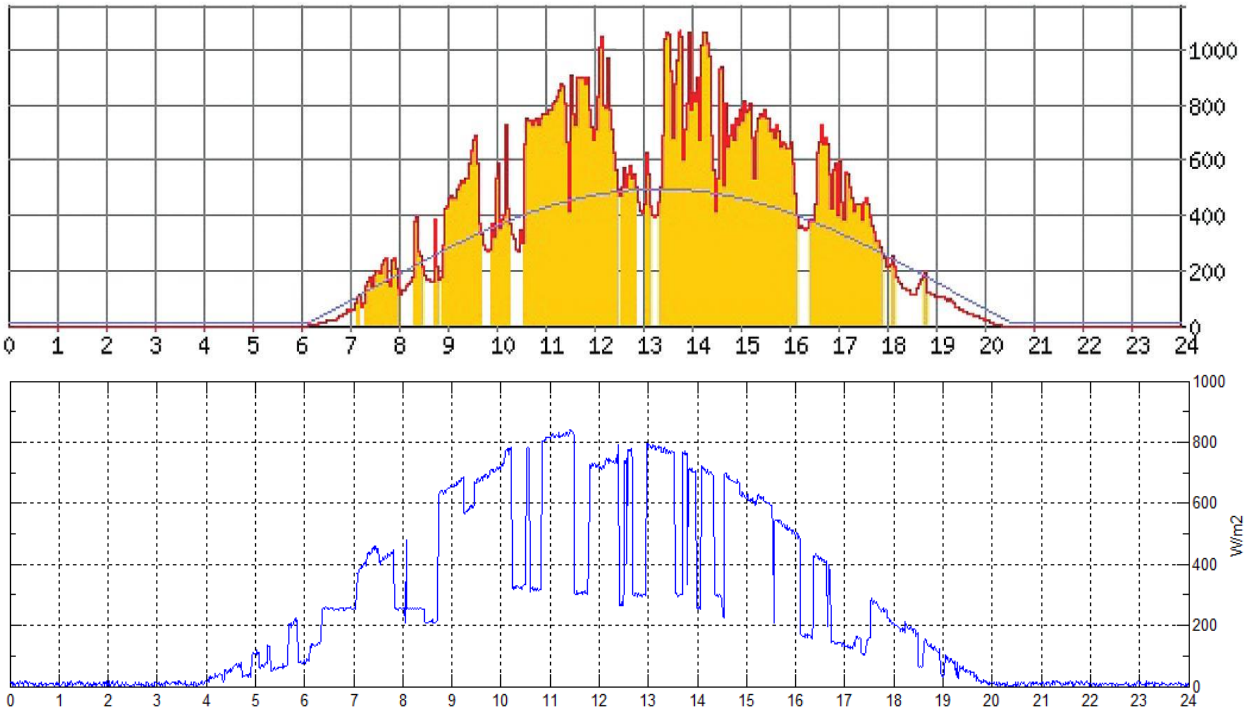

Figure 3.10. *Representation of real solar insolation in Lithuania (top) of solar insolation and simulated solar insolation in the model (bottom).*

3.4. Simulation of Photovoltaic module

Solar cells are usually grouped into "modules", which are encapsulated with various materials to protect the cells and the electrical connectors from the environment [7]. The manufactures supply PV cells in modules, consisting of N_{pm} parallel branches, each with N_{sm} solar cells in series. In practice solar panels manufacture will give limited characteristic parameters of solar panel, thus the suggested model can be established applying only standard manufacturer supplied data for the modules and cells. The solar module's current I^M can be described as:

$$I^M = I^M_{SC,op}\left[1-\exp\left(\frac{V^M - N_{SM}V^M_{OC,op} + R^M_S \cdot I^M}{N_{SM}V^C_t}\right)\right] \qquad 3.22.$$

The expression function of the PV module's current I^M is an implicit function, being dependent on: short circuit current of the module (2.23), open circuit voltage of the module (2.24), equivalent serial resistance of the module (2.25) and thermal voltage in the semiconductor of a single solar cell (2.26):

$$I_{SC}^{M} = N_{PM} I_{SC}^{C} \quad 3.23.$$

$$V_{OC}^{M} = N_{SM} V_{OC}^{C} \quad 3.24.$$

$$R_{S}^{M} = \frac{N_{SM}}{N_{PM}} R_{S}^{C} \quad 3.25.$$

$$V_{t}^{C} = \frac{mkT^{C}}{e} \quad 3.26.$$

$$P_{\max}^{C} = P_{\max}^{M} \left(N_{SM} / N_{PM} \right) \quad 3.27.$$

$$V_{OC}^{C} = V_{OC}^{M} / N_{SM} \quad 3.28.$$

$$I_{SC}^{C} = I_{SC}^{M} / N_{PM} \quad 3.29.$$

Under operating conditions solar cell characteristics are calculated accordingly:

$$I_{SC,op}^{C} = \left(I_{SC}^{C} / S_{\text{standard}} \right) \cdot S_{\sum} \quad 3.30.$$

$S_{\sum}$ - total solar irradiation (2.21) in operating point.

$$T^{C} = T_{ambient} + C_2 G_a \quad 3.31.$$

C_2 - 0.03 Cm^2 / W reasonable approximation described in *'Models for a stand-alone PV system'* [7]

$$V_{OC,op}^{C} = V_{OC}^{C} + C_3 \left(T^{C} - T_{0}^{C} \right) \quad 3.32.$$

C_3 - temperature coefficient of the cell ~-2.3 *mV/C.*

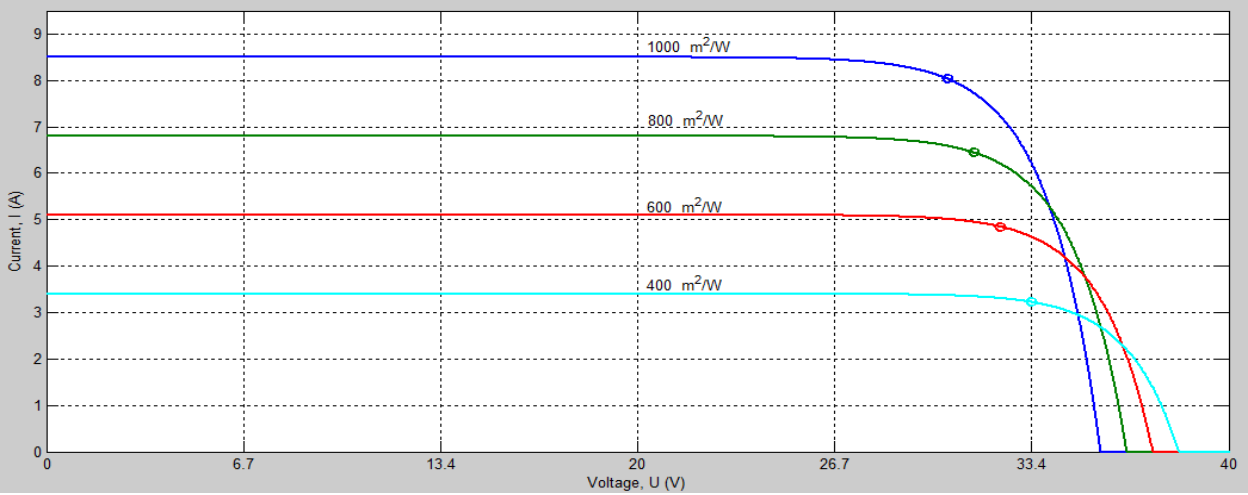

3.11 Figure. *I-V characteristics of Solet P60.6-230 under different solar insolation (blue – 1000 m^2/W, green – 600 m^2/W, red – 400 m^2/W, cyan – 400 m^2/W) in Vilnius area 54°N 25°E under 20°C ambient temperature*

In current practice, the performance of a module or another PV device is determined by exposing it at known conditions, for example standard conditions which is given by manufacturer. Solet P P60.6-230 is a PV module made by *AB „Precizika“* - one of the most known solar panels manufacturer in Lithuania with characteristics are presented in table III.

Table III

Solet P60.6-230 Specifications

P_{max}	V_{max}	I_{max}	V_{OC}^{M}	I_{SC}^{M}
230-235 W	*29.3 V*	*7.9 A*	*36.8 V*	*8.5 A*

This data were proven at standard conditions: Solar insolation – 1000 W/m^2, PV modules temperature – 25°C, air mass coefficient 1.5. In PV modules solar cells are connected in series to provide a reasonable voltage, thus Solet P60 has 60 pieces of polycrystalline solar cell connected in series. In table IV Solet P60.6-230 was executed under four different solar insolation with ambient temperature of 20°C.

As illustrated in Figure 3.11, peak power of photovoltaic module degrades to 107.83 W from nominal 246.12 W gaining loss of 56.18 % power. In Figure 3.12 photovoltaic module was exposed under different ambient temperatures. With increased temperature of PV module power, the I-V characteristic goes from right to left, thus the peak power is decreasing. The power of Solet P60.6-230 module degrades each 1.245 W with 1°C of temperature change.

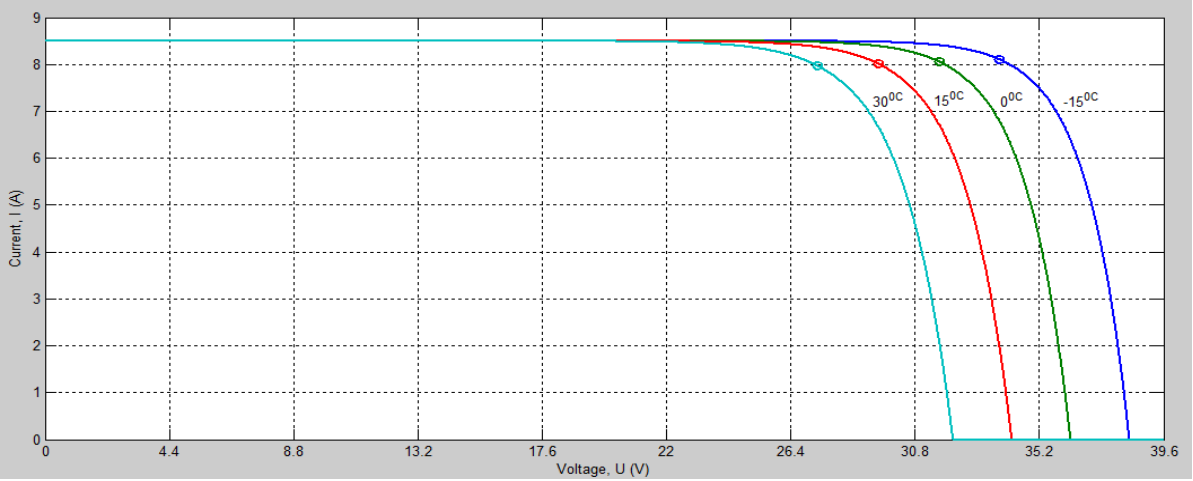

3.12 Figure. *I-V characteristics of Solet P60.6-230 under different temperature (blue – -15^{0C}, green – 0^{0C}, red – 15^{0C}, cyan – 30^{0C}) in Vilnius area 54°N 25°E under 1000 m^2/W of solar insolation*

Table IV

Solet P60.6-230 I-V characteristics under different solar insolation

Solar insolation	*Ambient temperature*	*V_{mpp}*	*I_{mpp}*	*P_{mpp}*
1000 m^2/W	*20^{oC}*	*30.65 V*	*8.03 A*	*246.12 W*
800 m^2/W	*20^{oC}*	*31.54 V*	*6.45 A*	*203.43 W*
600 m^2/W	*20^{oC}*	*32.45 V*	*4.85 A*	*157.38 W*
400 m^2/W	*20^{oC}*	*33.49 V*	*3.22 A*	*107.83 W*

Table V

Solet P60.6-230 I-V characteristics under different ambient temperature

Solar insolation	*Ambient temperature*	*V_{mpp}*	*I_{mpp}*	*P_{mpp}*
1000 m^2/W	*-15^{oC}*	*33.79 V*	*8.108 A*	*274.11 W*
1000 m^2/W	*0^{oC}*	*31.66 V*	*8.061 A*	*255.18 W*
1000 m^2/W	*15^{oC}*	*29.39 V*	*8.045 A*	*236.50 W*
1000 m^2/W	*30^{oC}*	*27.25 V*	*8.002 A*	*218.01 W*

The output characteristics when one shaded photovoltaic module is connected to the other non-shaded modules in series are illustrated in Fig. 3.13. The shading effect results in degraded module output because the current of the series-connected modules is affected by the shaded module. The same result will be if only one shaded cell which is the last one in module

connections is shaded, thus this has resulted in module manufactures employing bypass diodes to preserve array voltage and to minimize hot-spot heating and potential failures for cell when shaded. Table VI results show that when one shaded module is connected with three non-shaded modules in series the peak power decreases from 689.97 W to 585.09 W thus reducing power by 14.83 %. In this case it is more efficient to completely remove shaded module from array than to operate at partial capacity and degrade the performance of the other modules. More results about partial shading condition are described in next chapter.

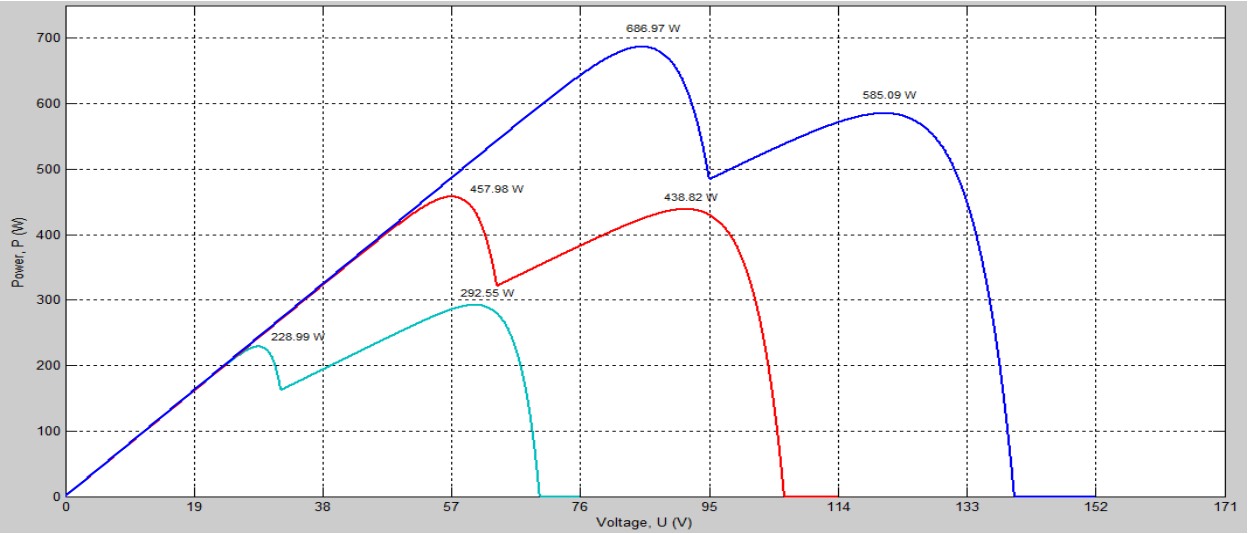

3.13 Figure. *P-V characteristics of Solet P60.6-230 connected in series with one shaded panel from 1000 m^2/W to 600 m^2/W of solar insolation. Blue – four series connected modules, red – three series connected modules, cyan – two series connected modules.*

Table VI

Losses caused by series-connected modules under one modules shaded condition

Number of series connections	*Unshaded insolation*	*Shaded insolation*	*Unshaded modules MPP*	*With shaded module MPP*	*Relative power change (%)*
Two modules	*1000 m^2/W*	*600 m^2/W*	*228.99 W*	*292.55 W*	*27.76 %*
Three modules	*1000 m^2/W*	*600 m^2/W*	*457.98 W*	*438.82 W*	*-4.18 %*
Four modules	*1000 m^2/W*	*600 m^2/W*	*686.97 W*	*585.09 W*	*-14.83 %*

3.5. Impact of partial shading on PV module

We consider the case when the cells in a module are all connected in series. Shading a single cell causes the current in the string of cells to fall to the level of the shaded cell [29]. Open circuit voltage of a silicon solar cell is around 0.6V. A solar module is constructed by connecting a number of cells in series to get a practically usable voltage. Partial shading of solar PV module is one of the main causes of overheating of shaded cells and reduced energy yield of the module [30].

Maximum power point tracking algorithm is widely implemented in photovoltaic system to maximize the PV array output power. In general, Pertrub and Observe is simple thus being selected to continuously track the array maximum power point. Under uniform solar, PV array characteristic is non-linear and consisting only one MPP along the functional operating voltage. However, when the PV array is partially shaded, the P-V characteristic becomes more complex with multiple MPPs. The occurrence of multiple MPP might cause the PV array to be trapped at the local MPP. At this operating condition of local MPP, PV array will generate lesser output power [31].

In any outdoor environment, the whole or some parts of the PV system might be shaded by trees, passing clouds, high building, etc., which result in non-uniform insolation conditions as it is shown in Figure 7.3. During partial shading, a fraction of the PV cells which receive uniform irradiance still operate at the optimum efficiency. Since current flow through every cell in a series configuration is naturally constant, the shaded cell needs to operate with a reverse bias voltage to provide the same current as the illumined cell. However, the resulting reverse power polarity leads to power consumption and a reduction in the maximum output power of the partially-shaded PV module. Exposing the shaded cell to an excessive reverse bias voltage could also cause “hotspots” to appear in them, and creating an open circuit in the entire PV module. This is often resolved with the inclusion of a bypass diode to a specific number of cells in the series circuit [32].

The modelling of the characteristic of PV array is based on superposition of each individual PV module characteristic. Theoretically, PV array will produce the same amount of generating current as the PV module which is operated under the same environmental conditions, on the other hand, the PV array provides greater output voltage. Referring to Fig. 3.14, the array

will gain three times operating voltage compared to the PV module. By-pass diode is externally coupled to each PV module to prevent hot spot formation in the PV array. During uniform solar illumination, the entire PV modules will generate the same amount of current. However, the shaded module will generate less current during PSC. The shaded module will cause the overall current generation by the entire PV array being limited. The solar cells will be reverse biased due to the mismatched effect and dissipate power in form of heat.

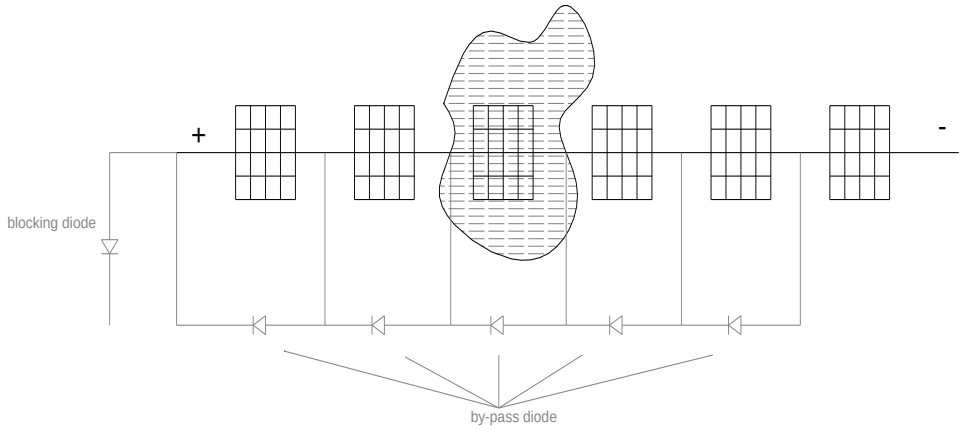

Figure 3.14. *Shading one of the PV module in the PV array system*

When the hot spots exceed the maximum power which can be sustained by the PV cells, it will cause permanent damage to the PV module and the array will be open circuited causing power interruption to the users. With by-pass diode, the excess current by the un-shaded PV module is allowed to flow through the external diode, preventing the PV module from being limited by shaded module and avoiding the destructive effect caused by hot spot formation in the PV array. Blocking diode is externally connected to the string of series connected PV modules. The function of blocking diode is to prevent the reverse flow of current particularly from the secondary power sources such as the lead-acid battery during the absence of sun light.

3.6. DC-DC voltage converter model simulation

DC-DC converter are widely used in photovoltaic generating systems as an interface between the photovoltaic panel and the load, allowing the follow-up of the maximum power point. Its main task is conditioning the energy generated by the array of cells following a specific control of strategy [33].

DC-DC converters are used in applications where a specific average output voltage is required, which can be higher or lower than the input voltage. This is achieved by exploring the times in which the converter's main switch (usually a MOSFET part) conducts to a varying frequency. The ratio of the time interval in which the switch is on (T_{ON}) to the commutation period (T_C) is called duty cycle (d) of the converter, which varies in the range from 0 to 1. By using switch mode control in the circuit in Fig. 3.15, the output voltage V_{out} will be constant pulse and the duty ratio will be $d=0.33$.

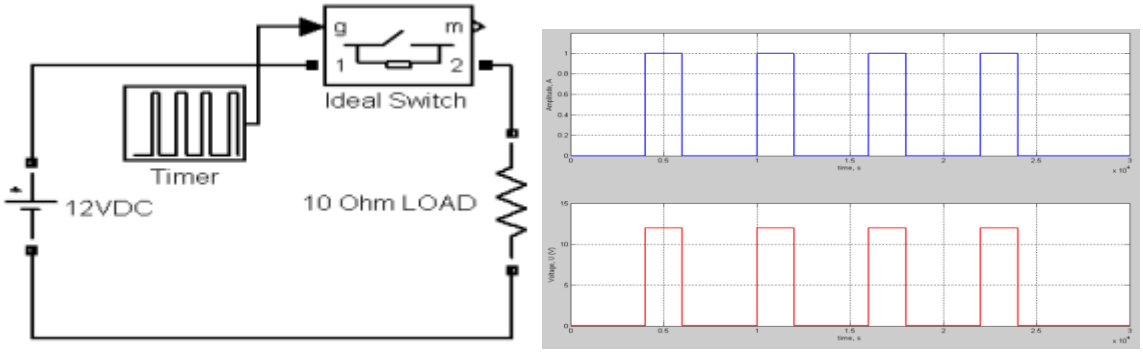

Figure 3.15. *Voltage source connected to ideal switch and a load. The output voltage of the circuit is pulse voltage with period equal to switch period. When switch is in on-state voltage drops across the load, when switch is off the load is cut-off from voltage supply.*

3.6.1. Buck type converter

The buck converter produces a lower DC voltage output than the input. The circuit can be seen in Fig. 3.16. This circuit is an improved version of the circuit in Fig. 3.15. The resistive load is

replaced by a diode to overcome the problem of stored inductive energy that will normally appear in the circuit.

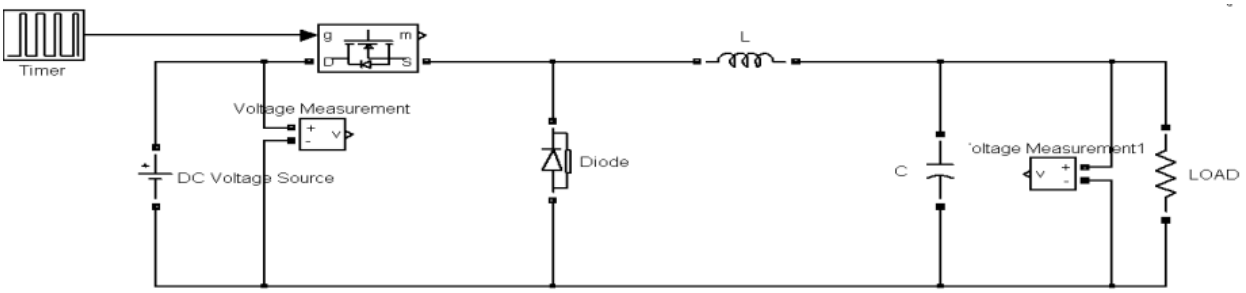

Figure 3.16. *Buck DC/DC converter Simulink circuit model*

Second part of the converter is the low-pass filter which reduces the output voltage fluctuations, this is achieved by selection of filter parameters to reduce the corner frequency.

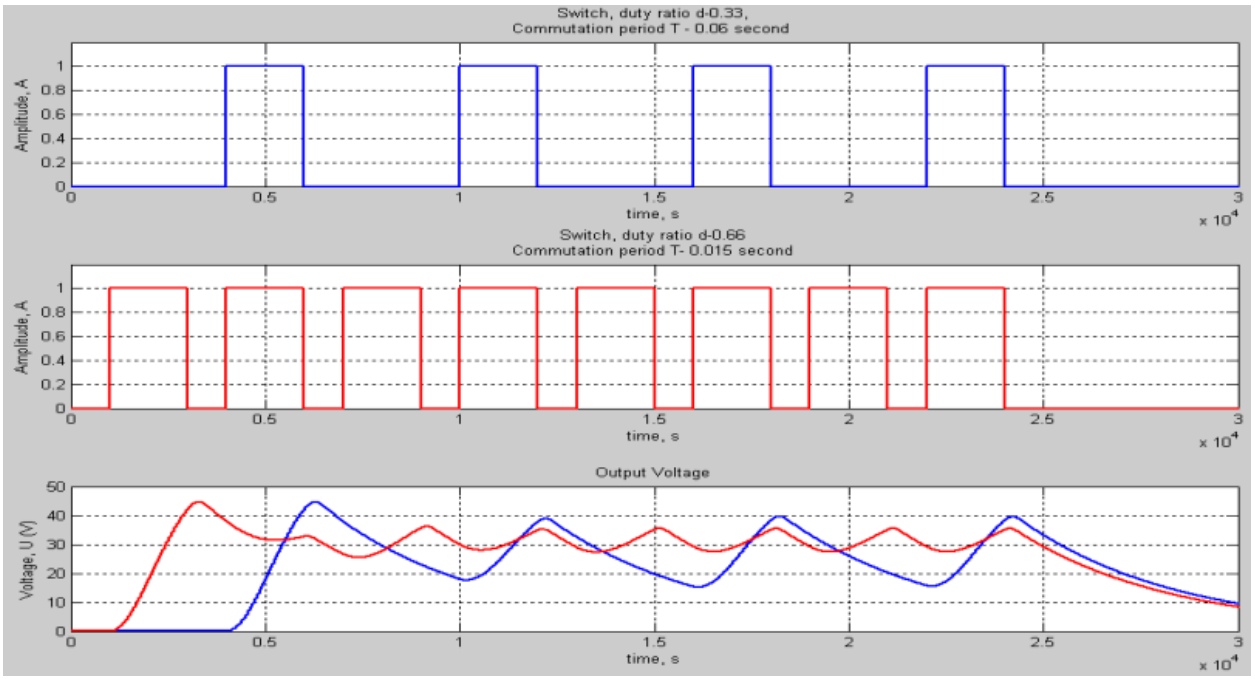

Figure 3.17. *Execution of buck type converter using different switch period and duty cycle*

As seen in Fig. 3.18, buck type converter decreases input voltage (V_{in}=*40 V*). Results show that when duty ratio (*d*) with commutation period of the switch is 0.33, the capacitor *C* is fast enough to discharge the voltage, thus gives the minimum of output voltage 16 V. When duty ratio is 0.66, the output voltage is more stable, thus if the requirements of the system is to get lower

voltage without any fluctuations duty ratio of the switch must be increased. In table VII. Are shown the component values of the buck converter

Table VII

Duty ratio comparison of a buck type converter

Duty ratio (d)	*Commutation period (T_C)*	*Inductor value (L)*	*Capacitor value (C)*	*Load resistance (R)*	*Voltage fluctuation (%)*
0.33	*0.06 s*	*1 mH*	*20 mF*	*1 ohm*	*62 %*
0.66	*0.03 s*	*1 mH*	*20 mF*	*1 ohm*	*20.8 %*

In order to minimize the component values such as *C=20 mF* capacitor rather choose to increase the switching frequency of the switch [34]:

$$f_c = \frac{1}{2\pi\sqrt{LC}} << f_s \qquad 3.33.$$

Whereas f_c is the cut-off frequency, f_s switching frequency of the switch. In this case our f_c = *113 Hz, where* f_{s1}*=16.7 Hz* and f_{s2}*=33.4 Hz.* In order to achieve great stability in the buck type converter and to minimize the capacitor value to C1=0.001 mF our switching frequency must be much higher than 5000 Hz.

3.6.2. Boost type converter

Boost type converter is opposite of a buck converter, which takes the input voltage and amplitudes that the output voltage would be higher. A boost type converter circuit modeled in Simulink is presented below in Fig. 3.18.

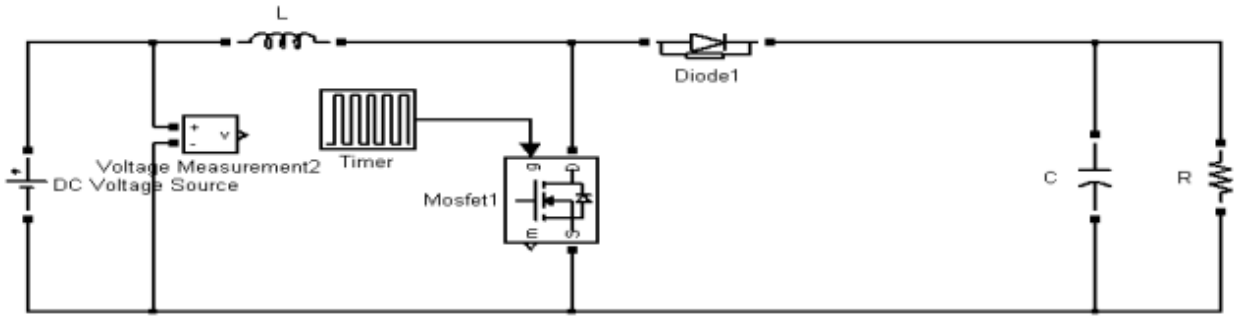

Figure 3.18. *Boost type converter circuit in Simulink*

As illustrated in Fig. 3.18 the MOSFET which is the circuit's switch is connected after the inductive element. When switch is in on-state, the output circuit is isolated from the supply. And the inductive element will generate inner inductive current, because it is supplied by the constant voltage source as given by the formula:

$$v_L = L\frac{di_L}{dt} \qquad 3.34.$$

When the switch is in off-state output circuit will be supplied by the constant voltage and by the inductive current which will decrease in time, thus in the output will get an increased voltage.

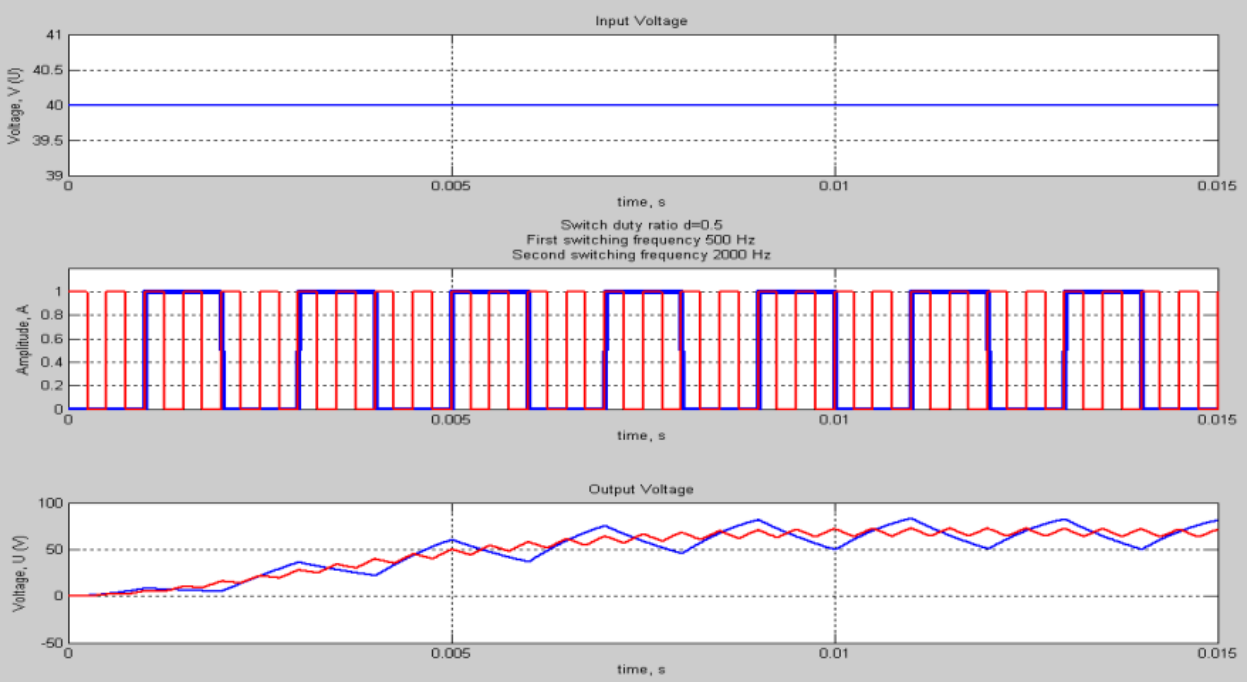

Figure 3.19. *Execution of a boost type converter with different switching frequency*

The boost converter's circuit element values, which were used for simulation presented in Fig. 3.19, are shown in Table VIII. As mentioned above, in buck type converter with switching frequency increase the output voltage fluctuations will be decreased.

Table VIII

Comparison of a boost type converter using different switching frequency

Duty ratio (d)	*Commutation period (T_C)*	*Inductor value (L)*	*Capacitor value (C)*	*Load resistance (R)*	*Voltage fluctuation (%)*
0.5	*0.002 s*	*1 mH*	*2 mF*	*1 ohm*	*39 %*
0.5	*0.0005 s*	*1 mH*	*2 mF*	*1 ohm*	*13.69 %*

3.6.3. DC/DC converter for photovoltaic module

The buck and boost converter topologies successfully changes the output voltage level according to different switching frequency and component values. In order to achieve maximum power point in photovoltaic module under variable climate conditions input voltage must be regulated. Simple solution could be an implementation of input capacitor in the DC-DC type converter which previously was investigated. After the input capacitor is connected in parallel with current source, the input voltage could be calculated as follows:

$$I_{pv} = C\frac{d}{dt}(V_{in}) \qquad 3.35.$$

$$\frac{I_{pv}dt}{C} = d(V_{in}) \qquad 3.36.$$

$$V_{in} = \int d(V_{in}) = \frac{I_{pv}}{C}\int dt = \frac{I_{pv}t}{C} + K \qquad 3.37.$$

Formula above (3.37) states that with constant current source the input voltage is proportional with the time that capacitor is discharges and inverse proportional to the capacitance value. The capacitor discharge time is equal to the switch period that is commutated with the circuit as shown in Fig. 3.20.

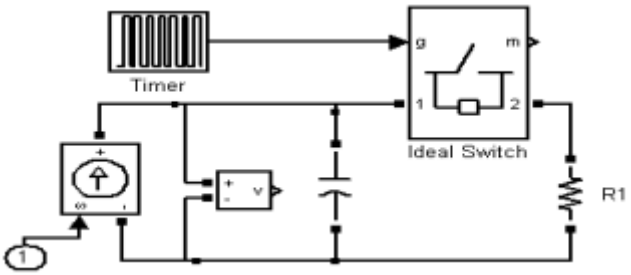

Figure 3.20. Basic circuit for controlling input voltage

Table IX

Input voltage characteristics under different commutation period

Duty ratio (d)	*Commutation period (T_C)*	*Capacitor value (C)*	*Current source amplitude*	*Input voltage minimum*	*Input voltage maximum*
0.5	*10^{-5}s*	*2 μF*	*7.4 A*	*9.03 V*	*27.32 V*
0.5	*10^{-6}s*	*2 μF*	*7.4 A*	*13.93 V*	*15.59 V*

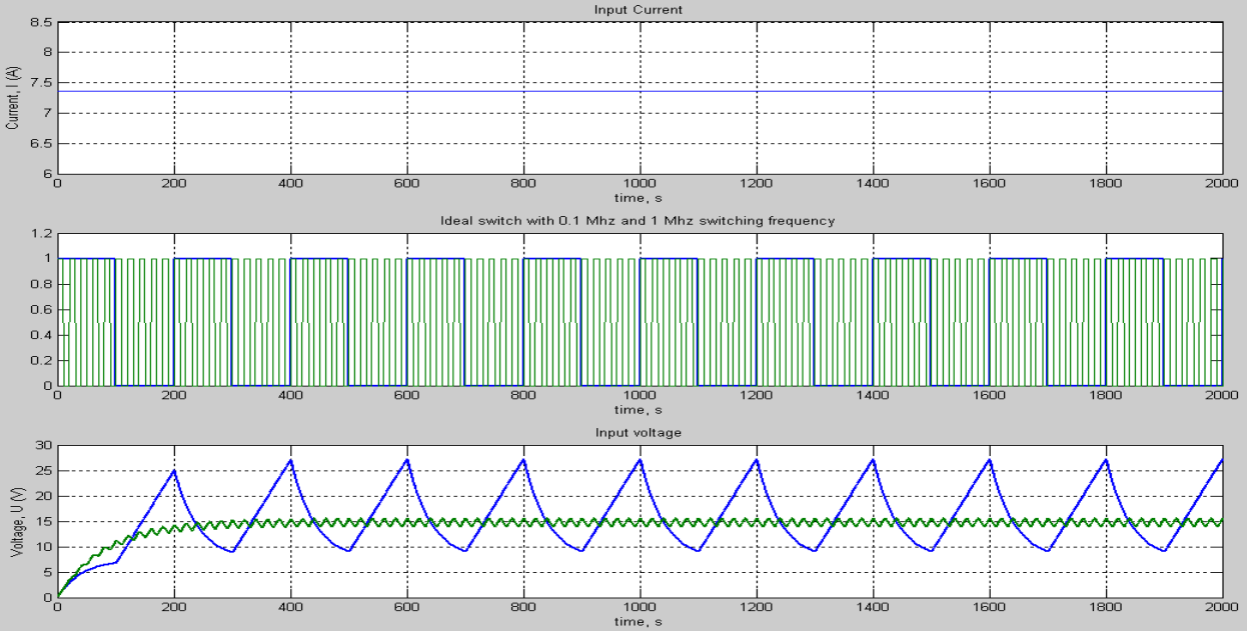

Figure 3.21. *Input voltage characteristics of basic controlling input circuit using different switching frequency (blue – 0.1 MHz, green – 1 MHz)*

As seen from the results, the input voltage could be controlled by using different switching frequencies of the switch, thus the increase of f_{switch} will give more stable input voltage. If the load in the basic input voltage controlling circuit is replaced with the buck or boost type DC-DC converter it could control the photovoltaic inputs voltage to the maximum power point voltage and give balanced DC voltage.

If the current source would be replaced with photovoltaic module, the maximum power point voltage could be regulated by the switch duty cycle. The testing results are given in Table X.

Table X.

Input voltage of photovoltaic module using different duty cycle of the switch

Duty ratio (d)	*Commutation period (T_C)*	*Capacitor value (C)*	*Current source amplitude*	*Input voltage*
0.2	*10^{-6}s*	*2 µF*	*7.4 A*	*Over 80 V*
0.4	*10^{-6}s*	*2 µF*	*7.4 A*	*40.86 V*
0.6	*10^{-6}s*	*2 µF*	*7.4 A*	*30.56 V*
0.8	*10^{-6}s*	*2 µF*	*7.4 A*	*23.21 V*

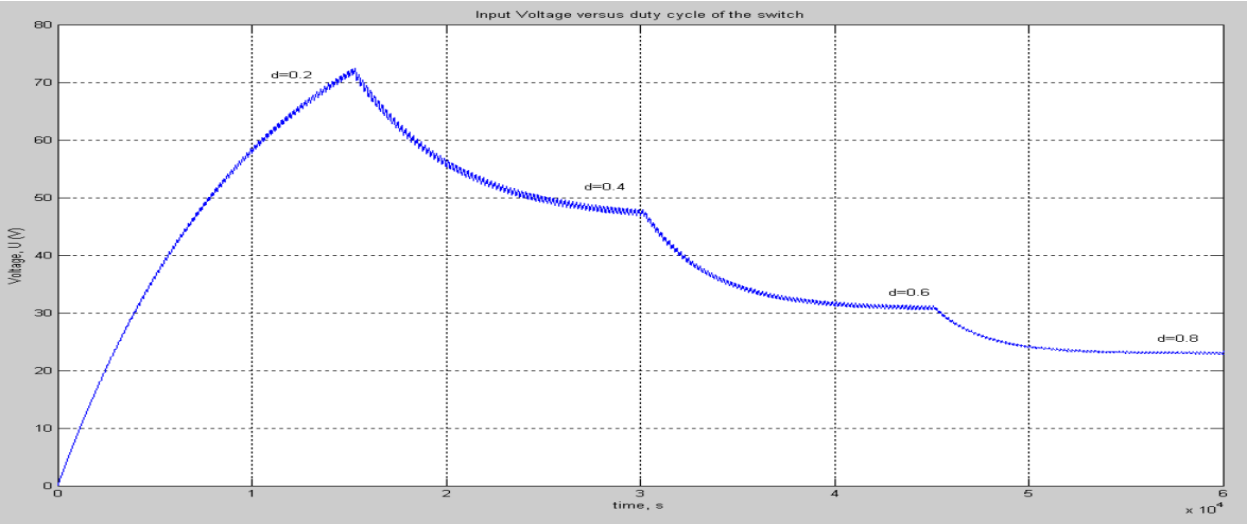

Figure 3.22. *Photovoltaic modules input voltage versus duty cycle of the switch*

Fig. 3.22 illustrates testing results presented in Table X. If the on-time of the switch will be lengthened the operating voltage of photovoltaic module will decrease. The results prove that capacitor connected in parallel and controlling is capable to control photovoltaic modules input voltage. If the load of the photovoltaic module will have only an active resistance the output voltage fluctuates from zero to operating voltage when the switch turns off and on, accordingly. In this case output circuit is needed to balance the output voltage to the nominal operating voltage of the photovoltaic module. The elements with reactive resistance such as inductor and capacitor are capable to store electric energy thus it is necessary to use them in output circuit of the DC-DC inverter.

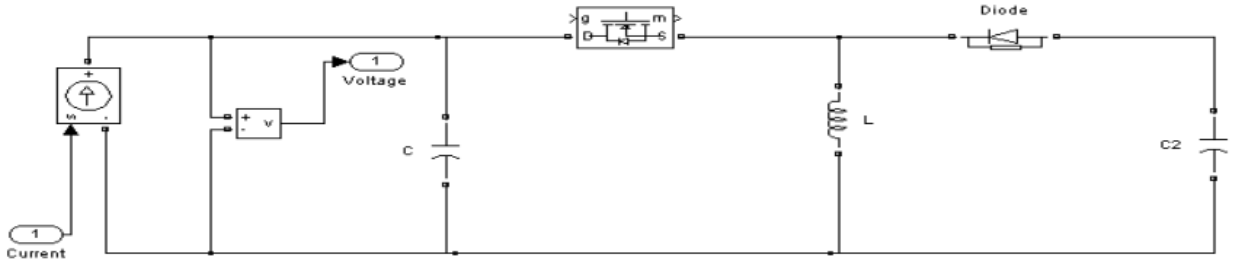

Figure 3.23. *Photovoltaic DC-DC converter with regulated output voltage*

The inductor on the output side of the circuit is able to store current for next switch pulse is made. The blocking diode is preventing current to flow to the load, thus evading the pulsed voltage fluctuations. Because of the blocking diode current will flow in reverse of the input circuit, thus will give negative output voltage. Below the Table XI shows the components and results of the simulation.

Table XI

Reactive element components which was used in Fig. 3.23 circuit

Duty ratio (d)	*Capacitor value (C)*	*Inductor value (L)*	*Capacitor value (C2)*
0.4	*40 µF*	*1 mH*	*40 µF*

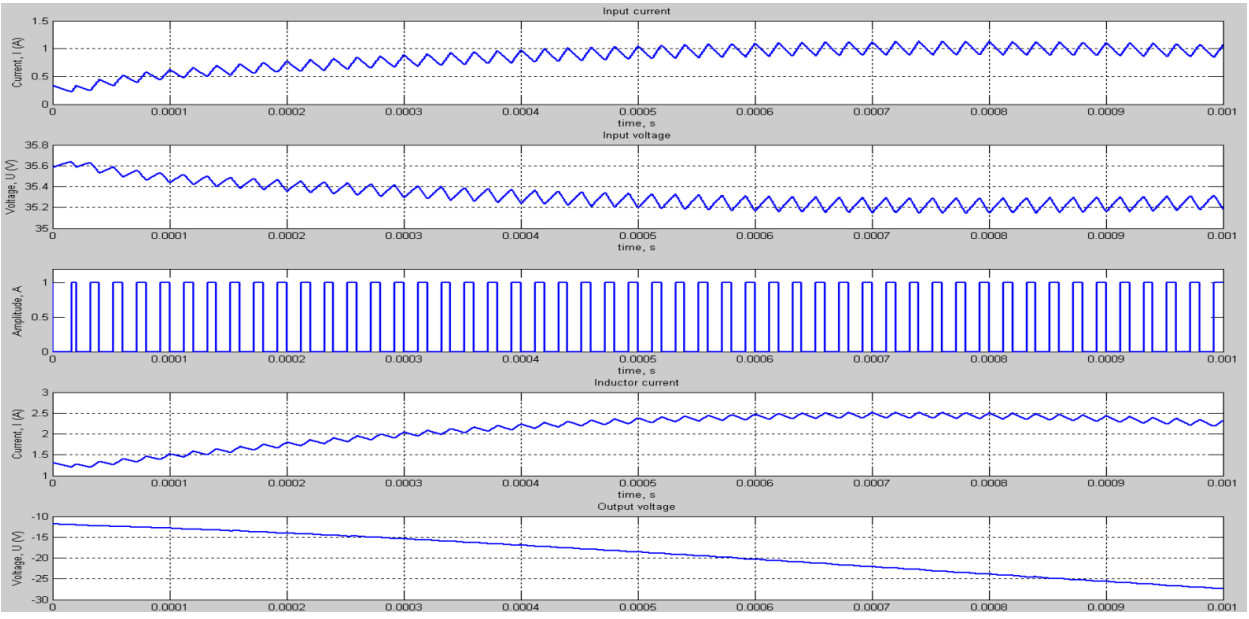

Figure 3.24. Photovoltaic modules voltage, current and power momentum

The type of converter that uses circuit in Fig. 3.24 is buck/boost which means the output voltage could be either lower or higher than the input voltage, it is only dependent on reactive component values and duty ratio of the switch. One of the main part of the circuit is the switch. It has to be integrated in DC-DC converter by a microcontroller. There are plenty of possible microcontrollers in the market at the moment, therefore, we will not investigate in more details the design of the switch. The next chapter will describe the structure of maximum power point algorithm.

4. Structure of MPPT algorithm

As mentioned in the Introduction part there are many maximum power point tracking algorithms with very less efficiency change, thus to check how complete circuit operates hill-climbing algorithm Fig. 4.1 is used.

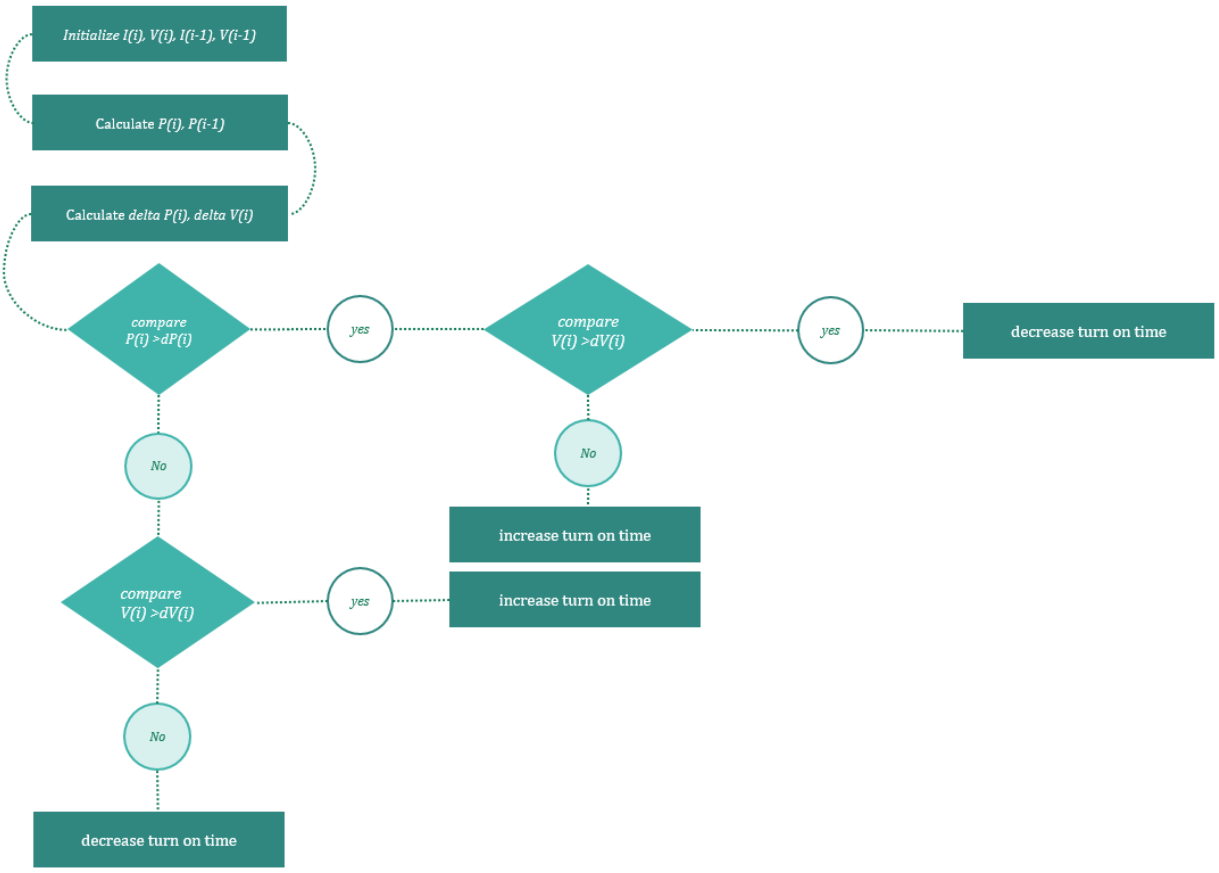

Figure 4.1. *Hill-climbing algorithm for photovoltaic maximum power point tracking application*

The first step is to proceed voltage and current values and memorize them. When next iteration voltage and current arrives, the existing power and previous power which was generated by the photovoltaic module, are calculated. After power calculation, the algorithm checks which is higher or lower than the previous power and makes a decision. If the existing power is lower than the previous it will compare voltages: if existing voltage is lower than previous switch turn on time must be decreased else opposite. Opposite selection is when existing power is higher than previous power. Below Fig. 4.2 illustrates results after algorithm implementation.

Table XII

Reactive element components which were used in circuit with MPPT

Temperature	*Insolation*	*Capacitor value (C)*	*Inductor value (L)*	*Capacitor value (C)*
25 ^{0C}	*800 m^2/W*	*4 mF*	*3 mH*	*4 mF*

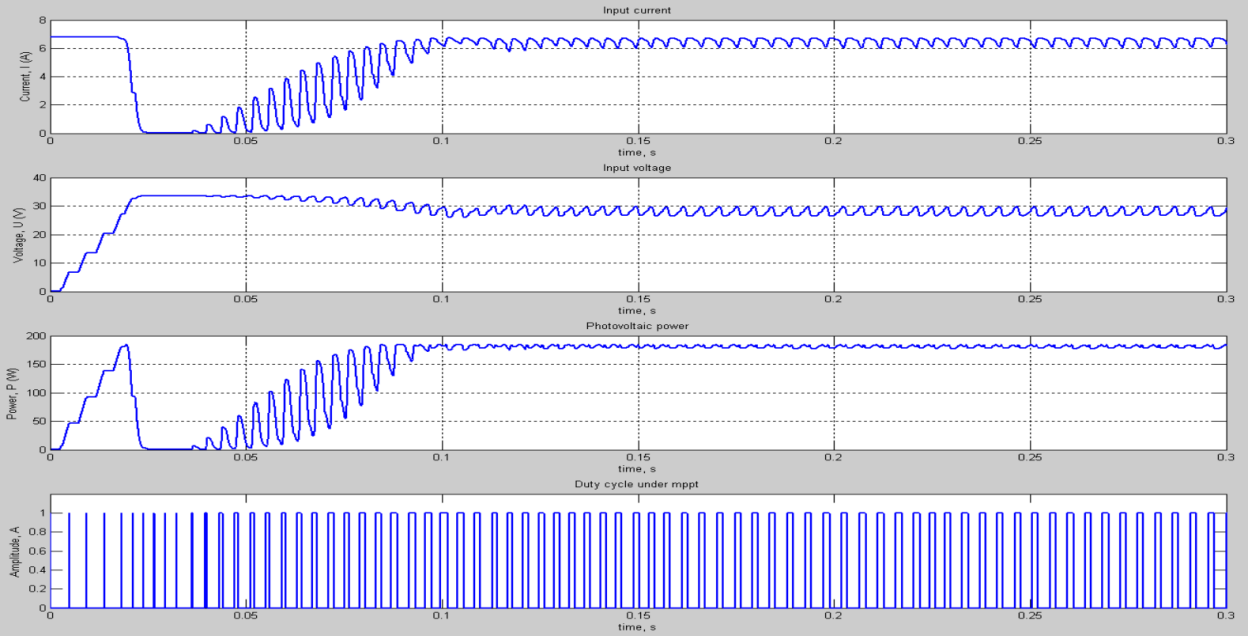

Figure 4.2. *Current, voltage and power of photovoltaic module change in time after the implementation of MPPT algorithm*

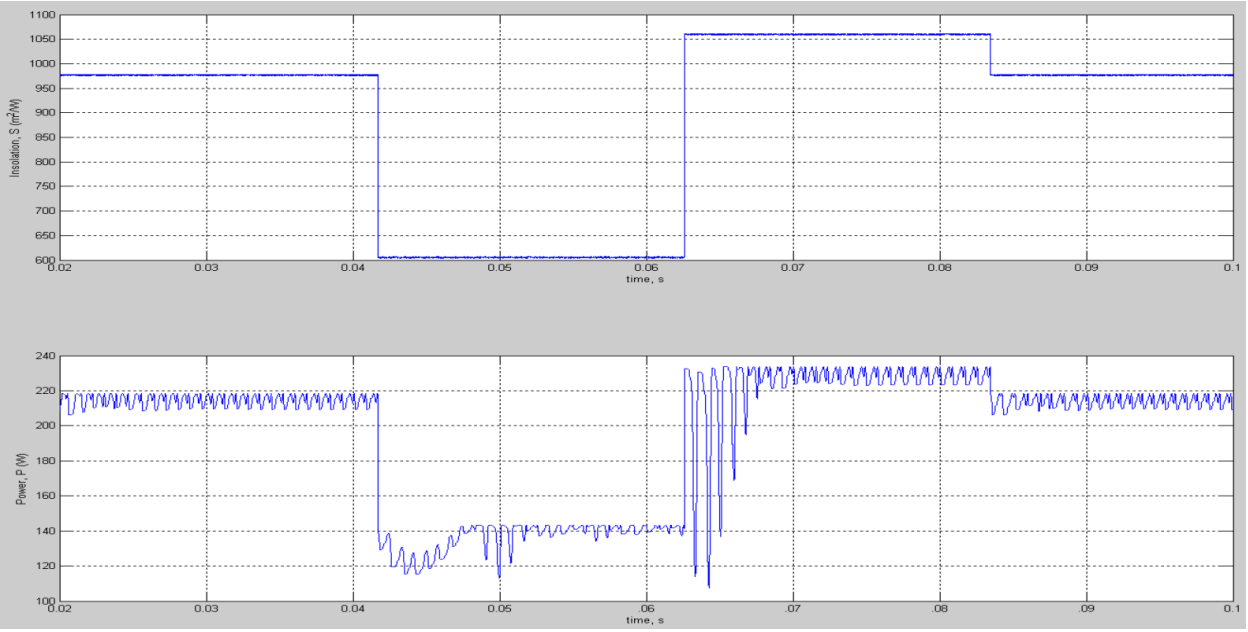

Figure 4.3. *Output power of photovoltaic module under fast variation of solar insolation*

At the beginning MPPT algorithm is not effective enough because of the small duty cycle ratio step. Open circuit voltage is reached, but after 0.1 s algorithm was capable to find maximum power point and fluctuates around it entire time. If the photovoltaic module would be exposed on a different solar insolation, PV power changes accordingly. Fig. 4.3 illustrates the results of output power of photovoltaic module being exposed under various insolation conditions. After 0.02s delayed from changed of insolation, the algorithm finds MPP and starts to fluctuate around it.

5. Comparison of generated power by photovoltaic using MPPT algorithm and without

The power generated by photovoltaic module with MPPT and with fixed load are presented in Table XIII.

Table XIII

Hour (h)	*Temperature* ^{0C}	*Insolation* m^2/W	*True MPP (W)*	*Hill-climbing MPP (W)*	*Fixed load (W)*
6	*15*	*40.93*	*10.77*	*10.42*	*1.77*
7	*16*	*74.64*	*19.64*	*19.02*	*3.19*
8	*17*	*252.65*	*66.44*	*64.34*	*17.11*
9	*17*	*413.08*	*106.15*	*103.19*	*45.72*
10	*19*	*255.82*	*67.25*	*64.06*	*17.54*
11	*21*	*676.61*	*167.22*	*159.34*	*122.64*
12	*23*	*332.68*	*86.49*	*82.43*	*29.65*
13	*25*	*729.15*	*178.77*	*167.05*	*142.33*
14	*26*	*720.84*	*176.96*	*164.62*	*139.12*
15	*26*	*764.19*	*186.37*	*172.96*	*156.15*
16	*22*	*670.99*	*165.97*	*157.71*	*120.61*
17	*24*	*583.89*	*146.32*	*137.24*	*91.35*
18	*21*	*168.88*	*44.94*	*39.69*	*7.64*
19	*20*	*169.88*	*45.21*	*39.92*	*7.73*
20	*19*	*155.32*	*41.41*	*36.49*	*6.46*
21	*17*	*46.06*	*12.12*	*11.74*	*1.99*

Comparison of power generated by photovoltaic module with MPPT and with fixed load

The data were gathered using the same reactive component values as in Table XII. Fixed resistance load – 3.7 *ohm*. Value for resistance load can be calculated using formula below:

$$R_{mpp} = \frac{U_{mpp}}{I_{mpp}} \qquad 3.38.$$

Where U_{mpp} and I_{mpp} are maximum power point voltage and current under 1000 m^2/W of solar insolation taken from Table I (*29.3 V, 7.9 A*). In reality fixed load R_{mpp} would be under solar insolation that exposes more frequently. True maximum power point is the highest value of P-V characteristic under specified solar insolation. Hill-climbing MPP is the median of 1 hour exposition of the specified solar insolation.

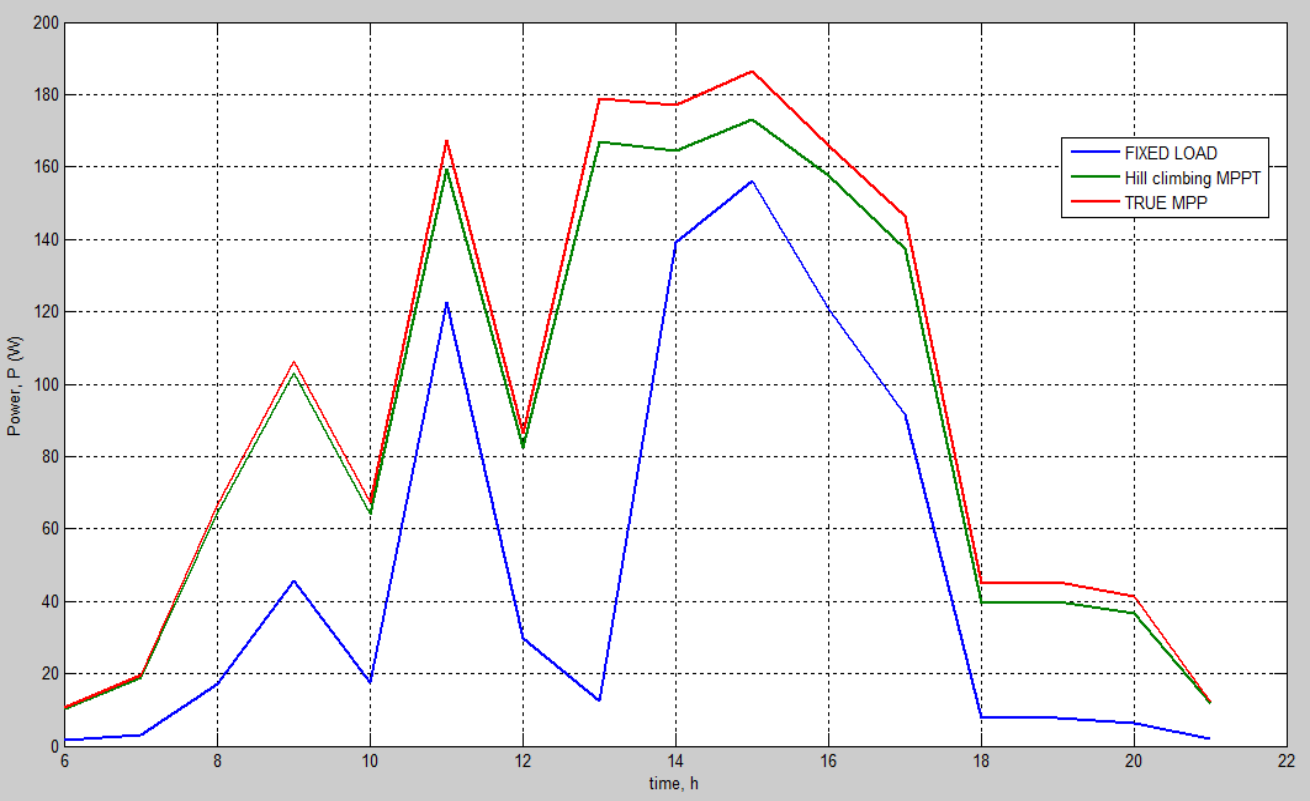

Figure 5.1. *Comparison of generated power by photovoltaic using MPPT algorithm and without*

As illustrated in Fig. 5.1 hill-climbing algorithm increases power generated by photovoltaic module. Table XIV expresses the percentage of all day generated power by 1 photovoltaic module with MPPT and with fixed load and compares them with true MPP.

Table XIV

True MPP	*Hill-climbing MPP*	*Fixed load*
1522 W	*1430 W*	*781 W*
100 %	*93.95 %*	*51.31 %*

Hill-climbing and fixed load generated power efficiency comparison

In Lithuania solar farms were not popular until government funded the price of 1 *kW/h* which is generated by photovoltaic modules. In comparison Table XV shows non-integrated and integrated in building roof solar generated electricity price which can be found in [37].

Table XV

Integrated Power (kW)	*Non-integrated (0.01 €)*	*Integrated (0.01 €)*
< 10	*15.65*	*20*
< 30	*14.20*	*17.97*
30 < IP < 100	*13.40*	*16.81*
100 < IP < 350	*13.40*	*16.81*
IP > 350	*13.40*	*16.81*

Solar generated electricity prices in Lithuania

For best economical revenue from photovoltaic generated electricity, 43 Solet P60.6-230 modules must be connected in series and parallel integrating totally of 9890 W. Losses between DC-AC inverter will be zero, thus for real example the losses must be calculated. Table XVI shows how much money will be in a day with described solar farm if every 43 of Solet P60.6-

230 photovoltaic module generates 1430 W per day, which will generate 61490 W totally and make 12.29 € revenue from government of Lithuania.

Table XVI

Revenue of solar generated electricity

Total integrated power	*Generated power*	*Revenue of the day*
9890 W	*61490 W*	*12.29 €*

6. Conclusions

1. Designed solar irradiation model is capable to produce full length of solar insolation in a specific location pointed by longitude and latitude and on a pointed day of the year starting from 1 (1^{st} of January) to 365 (31^{st} of December). The dependence of solar insolation (m^2/W) vs. time in hours (from 1 to 24) will be visualized in a graph. Adding a shading coefficient in cloudy day simulation enables to produce a more realistic solar insolation in Lithuania, thus it can be usable to produce research in neighbor countries: Latvia, Estonia, Poland, and Belarus.
2. Photovoltaic module simulation is capable to produce very realistic photovoltaic module with polycrystalline cells connected in series. Thus only slight change will be needed to implement different power modules into the system and compare them.
3. Selection of Buck/Boost topology allows to produce stable output voltage from photovoltaic module. It can be easily integrated in grid connected PV system only by connected with DC-AC inverter. Thus power transformation efficiency could be investigated, to get power losses from DC-AC inverter.
4. Designed switch in the DC-DC circuit makes possible MPPT. It uses Hill-climbing algorithm to turn on and off the switch with specified duty ratio. It enabled to reach 93.95% of efficiency comparing with true maximum power point.
5. Generated photovoltaic electricity shouldn't be a profit gaining source to private electricity sellers. It is renewable energy source that doesn't use any additional resources except solar insolation, thus it helps to stop climate change. In Lithuania nearly 10 kW of integrated power solar farm mounted on the building roof could produce 12-13 € profit per summer day.

7. References

[1] Pei Zhai, Eric D. Williams. (2011) 'Analyzing consumer acceptance of photovoltaic (PV) using fuzzy logic model', *Elsevier*, Renewable Energy 41, 2012, pp. 350-357.

[2] Vasarevičius D. (2012) ,Investigation andimprovement of eletronic control system for solar energy sources', *Vilnius Technika*, 2012.

[3] Chin C.S.,Neelakantan P., Yoong H. P., Teo K. T. K., (2011) ,Fuzzy logic based MPPT forphotovoltaic modules influenced by solar irradiation and cell temperature', UK Sim 13th International Conference on Modelling and Simulation.

[4] Lietuvos įstatymai. 2013. *Lietuvos įstatymai*. [ONLINE] Available at: http://www.istatymas.lt/istatymai/atsinaujinanciu_istekliu_energetikos_istatymas.htm. [Accessed 20 January 2013].

[5] Komisija patvirtino atsinaujinančių energijos išteklių gamintojams skatinamuosius tarifus 2013 metams . 2013. [ONLINE] Available at: http://www.regula.lt/lt/naujienos/index.php?full=yes&id=38798. [Accessed 20 January 2013].

[6] *Solar Power Vocab: Single & Dual Axis Solar Trackers :TreeHugger*. [ONLINE] Available at: http://www.treehugger.com/renewable-energy/solar-power-vocab-single-dual-axis-solar-trackers.html. [Accessed 21 January 2013].

[7] Nevzat O. (2010) 'Recent Developments in Maximum Power Point Tracking Technologies for Photovoltaic Systems', *Review Article*, International Journal of Photoenergy, Volume 2010, Article ID 245316, 11 pages.

[8] F.R.Rubio, M.G. Ortega, F.Gordillo, andM. L´opez-Mart´ınez,"Application of new control strategy for sun tracking," *Energy Conversion and Management*, vol. 48, no. 7, pp. 2174–2184,2007.

[9] Chin C.S.,Neelakantan P., Yoong H. P., Teo K. T. K., ,Optimisation of fuzzy based maximum power point tracking in PV system for rapidly changing solar irradiance', Global Journal of Technology&Optimization Volume 2, pp. 130–137 , 2011.

[10] *Fuzzy logic - Wikipedia, the free encyclopedia*. [ONLINE] Available at: http://en.wikipedia.org/wiki/Fuzzy_logic. [Accessed 21 January 2013].

[11] Fuzzification. 2013. *Fuzzification*. [ONLINE] Available at: http://www.atp.ruhr-uni-bochum.de/rt1/syscontrol/node122.html. [Accessed 21 January 2013].

[12] *Fuzzy rule-based systems*. [ONLINE] Available at: http://www.data-machine.nl/fuzzy1.htm. [Accessed 21 January 2013].

[13] [ONLINE] Available at: http://www.cs.bgu.ac.il/~sipper/courses/ecal051/lecon2.pdf. [Accessed 21 January 2013].

[14] Markvart, T., Castaner, L. 2003. Practical Handbook of Photovoltaics: Fundamentals and Applications. Oxford: Elsevier. 921 p. ISBN: 1856173909.

[15] D. Hansen, P. Sorensen, L. H. Hansen, and H. Bindner, *Models for a Stand-Alone PV System*, Danka Services InternationalA/S, 2001.

[16] H. Patel and V. Agarwal, "Maximum power point tracking scheme for PV systems operating under partially shaded conditions," *IEEE Transactions on Industrial Electronics*, vol. 55, no. 4, pp. 1689–1698, 2008.

[17] E. Karatepe, T. Hiyama, M. Boztepe, and M. C¸ olak, "Voltage based power compensation system for photovoltaic generation system under partially shaded insolation conditions," *Energy Conversion and Management*, vol. 49, no. 8, pp. 2307–2316, 2008.

[18] M.H. Taghvaee, M.A.M. Radzi, S.M. Moosavain, Hashim Hizam, M. Hamiruce Marhaban, ‚*A current and future study on non-isolated DC-DC converters for phtovoltaic applications*', Renewable and Sustainable Energy Reviews 17 (2013) 216-227.

[19] *The Earth's Elliptical Orbit Around the Sun - Aphelion and Perihelion*. [ONLINE] Available at: http://geography.about.com/od/physicalgeography/a/orbitsun.htm. [Accessed 31 January 2013].

[20] Freeman D., 'Introduction to Photovoltaic Systems Maximum Power Point tracking', *Texas Instruments*, Application report, November 2010. [ONLINE] Available at: http://www.ti.com/lit/an/slva446/slva446.pdf. [Accessed 22 January 2013].

[21] Esram T., Chapman P. L., 'Comparison of Photovoltaic Array Maximum Power Point Tracking Techniques', [ONLINE] Available at: http://energy.ece.illinois.edu/chapman/papers/EC%202006%20in%20press.pdf. [Accessed 22 January 2013].

[22] N. Khaehintung, K. Pramotung, B. Tuvirat, and P. Sirisuk, "RISCmicrocontroller built-in fuzzy logic controller of maximum power point tracking for solar-powered light-flasher applications," in *30th Annual Conf. of IEEE Ind. Electron. Society*, 2004, pp. 2673-2678.

[23] Dr. Khalil K. Muhammed, Marwan A. Abdulhameed, 'Design and Implementation of A Fuzzy Logic Based A Photovoltaic Peak Power Tracking Controller', Al-Rafidain Engineering, Vol.20, No. 5, October 2012.

[24] Abou El-MaatyMetwally "Modelling and Simulation of a Photovoltaic Fuel Cell Hybrid System", ph.D. Dissertation, Electrical Engineering University of Kassel, Kassel, Germany 2005. Ph.D.

[25] D. Vasarevicius, R. Martavicius, 'Solar Irradiance Model for Solar Electric Panels and Solar Thermal Collectors in Lithuania', *ISSN 1392 – 121, ELECTRONICS AND ELECTRICAL ENGINEERING, 2011. No. 2(108)*.Simoes, M. G., Franceschetti, N. N.

[26] Vasarevičius D. (2012) ,Investigation and improvement of eletronic control system for solar energy sources', *Vilnius Technika*, 2012.

[27] Zekai Sen, 'Solar energy fundamentals and modeling techniques : atmosphere, environment, climate change and renewable energy', 2008 Springer-Verlag London Limited, ISBN 978-1-84800-133-6.

[28] Claudy MC, Michelsen C, O'Driscoll A, Mullen MR. Consumer awareness in the adoption of microgeneration technologies an empirical investigation in the Republic of Ireland. Renew Sust Energ Rev 2010;14:2154e60.

[29] Chia Seet Chin, Prabhakaran Neelakantan, Soo Siang Yang, Bih lii Chua, Kenneth Tze Kin Teo, '*Effect of Partially Shaded Conditions on Photovoltaic Arrays Maximum Power Point Tracking*', ISSN: 1473-804x online, IJSSST, Vol.12, No.3.

[30] Mohammadmehdi Seyedmahmoudian, Saad Mekhilef, Rasoul Rahmani, Rubiyah Yusof, Ehsan Taslimi Renani, 'Analytical Modeling of Partially shaded Photovoltaic Systems', ISSN 1996-1073, *Energies* 2013,6,128-144.

[31] Silje Odland Simonsen, '*Development of a Grid Connected PV System for Laboratory Use*', Norwegian University of Science and Technology.

[32] R.Ramaprabha, Dr.B.L.Mathur, '*Impact of Partial Shading on Solar PV Module Containing Series Connected Cells'*, International Journal of Recent Trends in Engineering, Vol 2, No. 7, November 2009.

[33] Shading | PVEducation. 2014. Shading | PVEducation. [ONLINE] Available at:http://pveducation.org/pvcdrom/modules/shading. [Accessed 04 April 2014].Vilnius – Vikipedija. 2013. *Vilnius – Vikipedija*. [ONLINE] Available at: http://lt.wikipedia.org/wiki/Vilnius. [Accessed 11 February 2013].

[34] Anca D. Hansen, Poul Sorensen, Lars H. Hansen, Henrik Binder, 'MODELS FOR A STAND-ALONE PV SYSTEM', Riso National Laboratory, Rosklide, December 2000.

[35] K. K. Tse, Member, IEEE, M. T. Ho, Student Member, IEEE, Henry S.-H. Chung, Member, IEEE, and S. Y. (Ron) Hui, Senior Member, IEEE, '*A Novel Maximum Power Point Tracker for PV Panels Using Switching Frequency Modulation'* IEEE transactions on power electronics, VOL. 17, NO. 6, November 2002.

[36] J.M. Enrique, E. Duran, M. Sidrach-deCardona, J.M. Andujar '*Theoretical assesment of the maximum power point tracking efficiency of photovoltaic facilities with different topologies*', Solar Energy 81 (2007) 31-38, Available at: www.sciencedirect.com

[37] Renewable resources (in Lithuanian). Atsinaujinantys ištekliai. Tarifai. [ONLINE]. Available at: http://www.regula.lt/atsinaujinantys-istekliai/Puslapiai/tarifai.aspx. [Accessed 26 May 2014].

Appendix A. Matlab code for creating cloudiness coefficient

```
x=1:1440;
cloud=rand(1,1440);
for j=3:1440

    if (cloud(j-1)-cloud(j))^2<0.5;
        cloud(j-1)=cloud(j-2);
    else cloud(j-1)=cloud(j-1);
    end
    figure(2)
    subplot(2,1,1)
    plot(cloud)

end
```

```
%% Total irradiation with clouds
Stnc=Stn.*cloud;
for k=1:720
        if k<=300
    if Stnc(k+380)<100
        Stnc(k+380)=150;
    end
        end
        if k<=500
    if Stnc(k+380)<200
        Stnc(k+380)=250;
    end
        end
        if k<=721
    if Stnc(k+380)<100
        Stnc(k+380)=150;
    end
        end
end
Stnc=Stnc+(10*noise);
```

Appendix B. Simulink model